



King Saud University

Arabian Journal of Chemistry

www.ksu.edu.sa  
www.sciencedirect.com



REVIEW ARTICLE

# Insights into recent advances of chitosan-based adsorbents for sustainable removal of heavy metals and anions



Ahmed M. Omer<sup>a,\*</sup>, Rana Dey<sup>b</sup>, Abdelazeem S. Eltaweil<sup>c,\*</sup>,  
Eman M. Abd El-Monaem<sup>c</sup>, Zyta M. Ziora<sup>d,\*</sup>

<sup>a</sup> Polymer Materials Research Department, Advanced Technology and New Materials Research Institute (ATNMRI), City of Scientific Research and Technological Applications (SRTA-City), New Borg El-Arab City, P.O. Box: 21934, Alexandria, Egypt

<sup>b</sup> School of Chemistry and Molecular Biosciences (SCMB), The University of Queensland, Brisbane, QLD 4072, Australia

<sup>c</sup> Chemistry Department, Faculty of Science, Alexandria University, Alexandria, Egypt

<sup>d</sup> Institute for Molecular Bioscience, The University of Queensland, Brisbane, QLD 4072, Australia

Received 26 August 2021; accepted 1 November 2021

Available online 8 November 2021

## KEYWORDS

Bioadsorbent;  
Heavy metals;  
Nitrate anions;  
Phosphate anions;  
Water treatment

**Abstract** With globally increased human population and industrialization, the natural sources of water are reduced and then contaminated. Therefore, development of advanced technologies for the efficient water treatment is becoming of the scope of each of the nation. One of the cost-effective and well-known technologies for wastewater treatment is adsorption of contaminants by natural biopolymer like chitosan (CS) due to its unique features such as availability, biodegradability, biocompatibility, eco-friendly and low-cost production. However, CS suffers considerable limitations such as low adsorption capacity, low surface area and limited reusability. Thence, this review intended to provide an overview for recent advances of chitosan-based adsorbents that established better adsorption activities towards various hazard heavy metals, including: As(III), As(V), Cu(II), Cr(VI), Pb(II) and Cd(II) ions. In addition, the capabilities of chitosan-based adsorbents for the adsorptive removal of anions including phosphates and nitrates were discussed. Besides, the suggested adsorption mechanisms of these contaminants onto chitosan-based adsorbents and the research conclusions for the optimum conditions of the adsorption processes were explained in light of the currently reported studies. Furthermore, to emphasize the foremost research gaps and future potential trends that could inspire further researchers to find out the best solutions for water treatment problems.

© 2021 The Authors. Published by Elsevier B.V. on behalf of King Saud University. This is an open access article under the CC BY-NC-ND license (<http://creativecommons.org/licenses/by-nc-nd/4.0/>).

\* Corresponding authors.

E-mail addresses: [amomar@srtacity.sci.eg](mailto:amomar@srtacity.sci.eg) (A.M. Omer), [abdelazeemeltaweil@alexu.edu.eg](mailto:abdelazeemeltaweil@alexu.edu.eg) (A.S. Eltaweil), [z.ziora@uq.edu.au](mailto:z.ziora@uq.edu.au) (Z.M. Ziora).  
Peer review under responsibility of King Saud University.



Production and hosting by Elsevier

## Contents

1. Introduction . . . . .	2
2. Chitosan-based adsorbents . . . . .	2
3. Chitosan for heavy metals removal . . . . .	4
3.1. Removal of arsenic . . . . .	4
3.2. Removal of copper . . . . .	7
3.3. Removal of chromium . . . . .	9
3.4. Removal of Lead . . . . .	11
3.5. Removal of cadmium . . . . .	13
4. Removal of phosphate and nitrate . . . . .	15
4.1. Removal of phosphate anions . . . . .	16
4.2. Removal of nitrate . . . . .	17
5. Summery . . . . .	17
6. Conclusions . . . . .	18
6.1. Gap of knowledge and future perspectives . . . . .	18
Declaration of Competing Interest . . . . .	19
References . . . . .	19

## 1. Introduction

The rapidly escalating water pollution is a worldwide environmental problem that threatens the life of the inhabitants on the earth (Inyinbor Adejumoke et al., 2018). There are diverse sources of water pollution including the recent industrial development having double impacts, definitely economically prosperous for some countries, but questionably considering all the hazard and waste is produced globally (Goel, 2006; Jain et al., 2021). Accordingly, the delivery of a safe drinking water is an anxious affair worldwide with drastically reduced its quality by increased number of detected contaminants, including anions, dyes, oil spills, heavy metals and especially pharmaceuticals, especially nowadays in this turbulent time of COVID-19 (Zambrano-Monserrate et al., 2020). Therefore, the improvement of the wastewater treatment methods in currently ongoing research projects has been focused on the combination of previously introduced techniques, including ion exchange (Zhao et al., 2019); electrolysis (Ao et al., 2019), membranes separation (Sahebjamee et al., 2019), ultra-filtration (Li et al., 2021), reverse osmosis (Li et al., 2019), catalysis (El-Sibriui et al., 2019; Sallam et al., 2018; El-Monaem et al., 2021), sedimentation, coagulation/flocculation (Zou et al., 2021) and adsorption (Guo et al., 2021; Eltaweil et al., 2021). The later technique is considered an excellent choice for the adsorptive removal of various hazard contaminants owing to its fast kinetic, costless and highly efficiency (Eltaweil et al., 2020; Omer et al., 2020; Eltaweil et al., 2021; Eltaweil et al., 2020; Eltaweil et al., 2021; Ahmed et al., 2020; Saheed et al., 2020). Various adsorbent materials, such as silica gel, activated carbons, resins, metal-organic frameworks (MOFs), clays and polymers have been extensively applied for the removal of various pollutants from water bodies (de Souza et al., 2018; Dongre et al., 2019; Bouyahmed et al., 2018; Naz et al., 2018; Wang et al., 2022; Wang et al., 2015; Abdelfatah et al., 2021). Consequently, sustained researches have been intensively executed in order to find out effectual adsorbents with acceptable adsorption profiles (Eltaweil et al., 2020; Eltaweil et al., 2020; Eltaweil et al., 2020). Table 1 listed various adsorbent materials and their features for wastewater treatments (Kentish and Stevens, 2001; Crini, 2005; Crini, 2006; Bhattacharyya and Gupta, 2008; Vickers, 2017; Crini and Badot, 2011).

Regarding the economic feasibility and environmental significance, carbohydrate biopolymers such as cellulose, alginate and chitosan have been receiving excessive attention over the last twenty years as alternative efficient adsorbents (Russo et al., 2021; Gomez-Maldonado et al., 2019; Singha and Guleria, 2014; Asadi et al.,

2018). This is due to their outstanding advantages including their natural abundance, being ecofriendly, biodegradability, ease of modification and low-cost production (Tamer et al., 2018; Khalifa et al., 2019). Several studies have been conducted regarding the adsorption aptitude of biopolymers-based adsorbents towards various heavy metals, toxic dyes, phenolic compounds, pharmaceutical residues and oil spills (Wang and Zhuang, 2017; El-Sayed et al., 2016; Omer et al., 2019; Kyzas et al., 2013; Eltaweil et al., 2021). Among these biopolymers, chitosan is a most prevalent, environmentally favored carbohydrate biopolymer with tremendous properties (Wang et al., 2018).

In the present review, we focus on the recent developments for boosting the adsorption capacity and reusability of chitosan-based adsorbents for efficient removal of the most prevailing heavy metals; As(III), As(V), Cu(II), Pb(II), Cd(II) and Cr(VI). In addition, the adsorption aptitude of the developed chitosan-based adsorbents towards the most deleterious anions; phosphate and nitrate anions were clearly investigated. The efforts that have been performed for improving their adsorption properties as well as their probable adsorption mechanisms and reusability were demonstrated. Furthermore, parameters affecting their adsorption performances were inspected. The research conclusions for the optimum conditions of the adsorption processes of these hazard pollutants were discussed and summarized. Finally, gap of knowledge and the future directions of chitosan-based adsorbents were offered.

## 2. Chitosan-based adsorbents

Chitin, the most abundant biopolymer in nature after cellulose, is the main constituent of the exoskeleton of arthropods and crustacean shells such as, and also is found in the cell walls of fungi as illustrated in Fig. 1 (Sandeep et al., 2013; Islam et al., 2011; Rinaudo, 2006; Al Sharabati et al., 2021). In 1859, chitosan has been obtained for the first time by Rouget, by boiling chitin in concentrated potassium hydroxide (Muzzarelli and Tanfani, 1985). Thereafter, chitosan has been firstly named by Hoppe-Seyler in 1894. Chitosan is an amino-polysaccharide that can be produced by N-deacetylation of chitin that involves the formation of amine groups ( $-\text{NH}_2$ ) from acetamide groups ( $-\text{NHCOCH}_3$ ) (Tamer et al., 2015; Zargar et al., 2015; Vakili et al., 2019; Tamer et al., 2015).

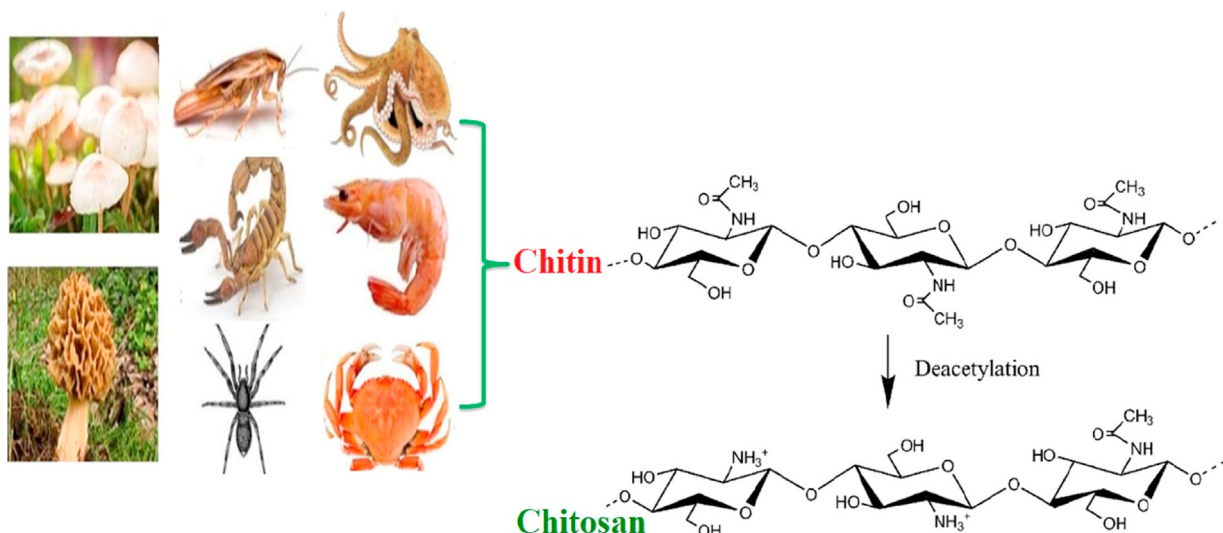
**Table 1** Different adsorbents (conventional and non-conventional) for the removal of pollutants from aqueous system and wastewaters.

Adsorbent	Features	Ref.
<b>Conventional adsorbents</b>		
Wood waste	Good surface phenomenon and efficient for large scale of pollutants.	(Tan et al., 2019)
Agricultural waste	Rapid and efficient.	(Dai et al., 2018)
Coconut shells waste	Used in granular form and widely used for wastewater treatment.	(Rahim et al., 2020)
Activated alumina	Commercially available and effective for bacteria, and organic matter removal.	(Kumari et al., 2020)
Silica gel	Efficient for removing of organic material (toluene, xylene, and acid dyes).	(Xu et al., 2018)
Zeolites	High ion exchange capacities and good adsorbents for dyes and organic solvents.	(Kobayashi et al., 2020)
Resins	Used for water treatment process.	(Nakakubo et al., 2019)
Cross-linked polymers	Regular spheroids with high surface area, high mechanical strength and chelating properties.	(Hu et al., 2019)
<b>Non-Conventional adsorbents</b>		
Solid waste from forest industries	Cheap and effective for many pollutants, possible regeneration.	(Silva et al., 2020)
Hydrogel	Effective for certain types of metal recovery.	(Duman et al., 2020)
Biomass from microorganism	Effective and more selective than ionic adsorbent.	(Kalaimurugan et al., 2020)
Polysaccharide derivatives	Cost effective, selective adsorption.	(Qi et al., 2018)
Chitin/chitosan Chitosan based derivatives	Biodegradable, renewable, abundant, cheap.	(Ngah et al., 2011)
	Cost effective biopolymer, available in gels, bids, powder and fibers. Exemplary diffusion properties, regenerative, useful for recovery of metals, dyes, oil spill recovery, and toxic pharmaceutical removal. High swelling capacity in water.	(Zhao et al., 2018)

Due to the unique features of chitosan such as polyelectrolyte properties, biocompatibility, hydrophilicity, adhesion properties, biodegradability and recyclability, chitosan has acquired a vast deal of concern in versatile biomedical, water treatment, cosmetics and food sectors as displayed in Fig. 2. In particular, chitosan has been considered as a promising cationic adsorbent for removing of anions, heavy metals, toxic organic dyes, aromatic compounds, oil spills and pharmaceuti-

cal residues (Omer et al., 2019; Solano et al., 2021; Liakos et al., 2021; Mu et al., 2020; Tanhaei et al., 2020; Asgari et al., 2020).

Chitosan possesses fabulous advantages including biodegradability, biocompatibility, high reactivity, hydrophilicity and nontoxic (Omer et al., 2021). In addition, chitosan is a linear polyamine structure with a number of free amine groups that are available for crosslinking and modification

**Fig. 1** Different sources of chitosan biopolymer.

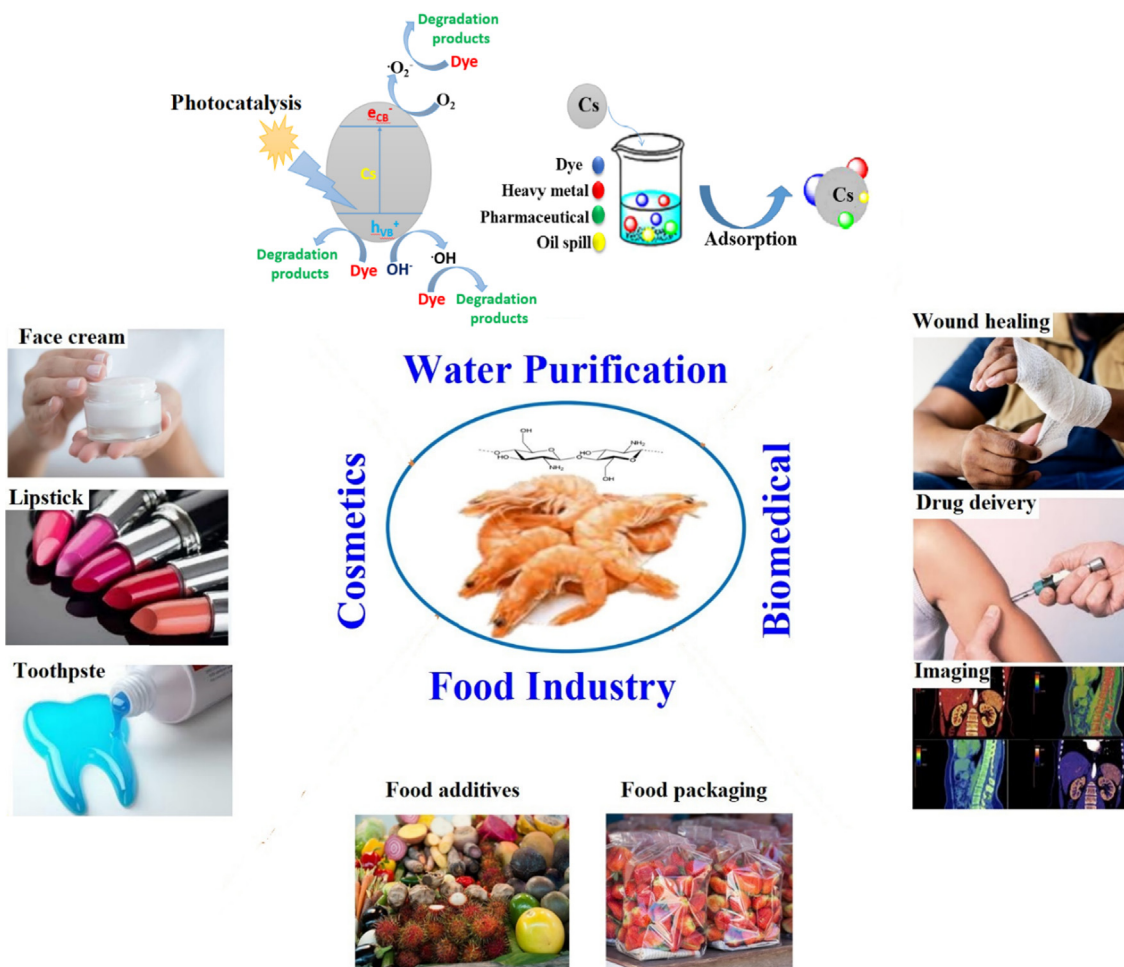


**Fig. 2** Various applications of chitosan biopolymer.

(Eldin et al., 2015). Nonetheless, chitosan has some flaws such as low water resistance, limited specific surface area, the incomplete recovery after adsorption process, poor mechanical and thermal properties, high tendency to agglomerate and high solubility in acidic conditions (Karimi-Maleh et al., 2021; Eltaweil et al., 2021; Wu et al., 2010). Therefore, several physical and chemical modification techniques including sulfonation, carboxymethylation and amination, in addition to schiff base formation, composite and grafting, have been conducted for neat chitosan to improves its adsorption characteristics and selectivity towards the removal of various toxic effluents from water (Kyzas et al., 2013; Kyzas and Bikaris, 2015; Eltaweil et al., 2021; Shebl et al., 2018; Shankar et al., 2014; Yuvaraja et al., 2020).

### 3. Chitosan for heavy metals removal

Chitosan is an excellent candidate for adsorbing the toxic metal ions from an aqueous solution as it possesses multiple chelation sites and amino and hydroxyl groups that attract the metal ions via coordination bond or ion exchange (Kaushal and Singh, 2017; El-saied and Motawea, 2020; Zhang et al., 2016; Zhang et al., 2019). Many studies have

focused on evaluating the adsorption property of chitosan and its modified forms towards their application for the removal of various heavy metals (Upadhyay et al., 2020; Yang et al., 2019; Wang et al., 2019; Gokila et al., 2017; Upadhyay et al., 2021). Table 2 summarizes some recent studies of the adsorptive removal of diverse heavy meals onto chitosan-based adsorbents.

#### 3.1. Removal of arsenic

Arsenic (As) is a pervasive element exists in the soils, air, rocks, water and organisms. It has been released into the environment through a combination of natural processes such as weathering reactions, biological actions, emissions and anthropogenic activities (Mandal and Suzuki, 2002). Arsenic is one of the multivalent heavy metals that cannot be readily removed and it converts into diverse forms or combines with other elements to form insoluble products (Choong et al., 2007). The most abundant oxidation states of arsenic ions are As(V), As (III) which are mostly in their oxyanions forms. Arsenite ( $\text{NaAsO}_2$ ) and arsenate ( $\text{Na}_2\text{HAsO}_4$ ) are the most predominant and both are highly toxic to living being (Sodhi et al., 2019). In addition,  $\text{H}_2\text{AsO}_4^-$  is the predominant at  $\text{pH} < 6.9$

**Table 2** Various chitosan-based adsorbents designed for removing of several heavy metals from aqueous solutions.

Absorbent	Adsorbate	$q_m$ (mg.g <sup>-1</sup> )	Ref.
Iron CS Microspheres	As(V)	120.7	(Lobo et al., 2020)
Magnetic CS Coated GO	As(III)	45.0	(Sherlala et al., 2019)
Zeolite/CS nanocomposite membrane	As(III)	N/A	(Mukhopadhyay et al., 2019)
CS Coated magnetite	As(III)	10.5	(Abdollahi et al., 2015)
Iron–chitosan composites	As(V)	22.5	(Gupta et al., 2009)
Iron–CS composites	As(III)	16.2	(Gupta et al., 2009)
Magnetic nanoparticles impregnated CS beads	As(V)	35.7	(Wang et al., 2014)
CS coated magnetite nanoparticle	As(V)	10.8	(Gogoi et al., 2017)
Fe(III)-chitosan	As(III)	19.7	(Pincus et al., 2021)
$\alpha$ -FeO(OH)/GO/CS	As(III)	289.4	(Shan et al., 2020)
MMT/CS	As(V)	3.4	(Cho et al., 2012)
Amidoxime-Functionalized CS	Cu(II)	190.7	(He et al., 2021)
Magnetic bentonite/Carboxymethyl CS/SA hydrogel beads	Cu(II)	56.8	(Zhang et al., 2019)
Zeolite X/CS hybrid microspheres	Cu(II)	152.0	(Lu et al., 2015)
Silica/CS composite	Cu(II)	870.0	(Gandhi and Meenakshi, 2012)
CNTs-CHO-CS composite	Cu(II)	115.8	(Dou et al., 2019)
CS-g-MA composite	Cu(II)	312.4	(Ibrahim et al., 2019)
CS/PVA/PEI membrane	Cu(II)	86.1	(Sahebjamee et al., 2019)
CS-g-PAA/APT	Cu(II)	303.03	(Wang et al., 2009)
CS-MMT hydrogel	Cu(II)	132.74	(Ngwabebhoh et al., 2016)
DTPA-CS/PEO nanofibers	Cu(II)	177.0	(Surgutskaia et al., 2020)
CS/TEOS/APTES nanofiber	Cu(II)	640.5	(Sabourian et al., 2016)
TEPA/CS/CoFe <sub>2</sub> O <sub>4</sub> composite	Cu(II)	168.06	(Fan et al., 2017)
Fe <sub>3</sub> O <sub>4</sub> @SiO <sub>2</sub> -CS composite	Cr(VI)	96.2	(Jiang et al., 2018)
Magnetic ZIF-67 MOF@Am-CS Beads	Cr(VI)	119.1	(Omer et al., 2021)
Chitosan–Fe(III) complex	Cr(VI)	173.1	(Shen et al., 2013)
Fe <sub>3</sub> O <sub>4</sub> / SiO <sub>2</sub> /CS-TETA composite	Cr(VI)	254.6	(Wang et al., 2020)
CS-MnO <sub>2</sub> nanocomposite	Cr(VI)	61.56	(Dinh et al., 2020)
CA-Polycaprolactone/CS nanofibers	Cr(VI)	126.0	(Ma et al., 2019)
CS/Montmorillonite–Fe <sub>3</sub> O <sub>4</sub> microsphere	Cr(VI)	58.8	(Chen et al., 2013)
CS/g-C <sub>3</sub> N <sub>4</sub> /TiO <sub>2</sub> nanofibers	Cr(VI)	68.9	(Li et al., 2021)
Nanobentonite/Nanocellulose/CS Aerogel	Cr(VI)	98.9	(Shahnaz et al., 2020)
Citrate-crosslinked Zn-MOF/CS composite	Cr(VI)	225	(Niu et al., 2021)
Alginate/Melamine/CS aerogel	Pb(II)	1331.6	(Gao et al., 2021)
polydopamine modified CS aerogels	Pb(II)	441.2	(Guo et al., 2018)
Magnetic-CS–PAA nanocomposite	Pb(II)	204.9	(Hu et al., 2020)
PEI-grafted magnetic CS microspheres	Pb(II)	134.9	(Sun et al., 2013)
CS-pectin gel beads	Pb(II)	266.5	(Shao et al., 2021)
Crosslinked carboxylated CS/ carboxylated nanocellulose hydrogel beads	Pb(II)	334.9	(Xu et al., 2021)
Hydroxyapatite/CS composites	Pb(II)	132.1	(Park et al., 2015)
CS-PVA nanofibers	Pb(II)	266.12	(Karim et al., 2019)
MnO <sub>2</sub> /CS nanoparticles	Pb(II)	126.1	(Dinh et al., 2018)
sodium tripolyphosphate cross-linked CS beads	Cd(II)	99.8	(Babakhani and Sartaj, 2020)
CS-based hydrogels	Cd(II)	234.8	(Vilela et al., 2019)
Vermiculite blended CS	Cd(II)	169.0	(Prakash et al., 2017)
Thiourea-modified magnetic ion-imprinted CS/TiO <sub>2</sub>	Cd(II)	256.4	(Chen et al., 2012)
CS/PVA/PEI membrane	Cd(II)	11.1	(Sahebjamee et al., 2019)
Hydroxyapatite/CS composites	Cd(II)	81.1	(Park et al., 2015)
CS-pectin gel beads	Cd(II)	177. 6	(Shao et al., 2021)
Cobalt ferrite@SiO <sub>2</sub> -CS/EDTA composite	Cd(II)	127.79	(Wang et al., 2020)
CS@NZVI	Cd(II)	142.80	(Ahmadi et al., 2017)
CS-VMT composite	Cd(II)	58.48	(Chen et al., 2018)

in the oxidizing conditions, whilst arsenite exists as HAsO<sub>4</sub><sup>2-</sup> at pH > 6.9 with the possibility of the presence of both H<sub>3</sub>AsO<sub>4</sub> and AsO<sub>4</sub><sup>3-</sup> at extremely acidic and alkaline medium, respectively. However, arsenite species are major forms under reducing conditions (Yan et al., 2000).

The most common sources for water pollution with such noxious pollutants are glassware fabrication, papers, pulp, cement and pharmaceutical industries (Adeloju et al., 2021; Shaji et al., 2020). Therefore, high concentrations of As cause

adversely impacts on human health such as problems with blood vessels, cancer, high blood pressure, heart disease, cardiovascular disease and skin lesions (Council, 1999; Robertson, 1989; Smedley and Kinniburgh, 2002; Podgorski and Berg, 2020). Thus, the exposure limit of As in drinking water has been reduced by World Health Organization (WHO) in 1993 from 50 to 10 µg l<sup>-1</sup> (Gao et al., 2021). This new recommendation is due to the growing awareness of the As toxicity, so As-contaminated water is a worldwide issue

and has become a critical challenge for scientists, engineers, and most policy makers.

Till date, many advanced adsorbents (e.g., carbon nanotubes, metal-organic frameworks, biopolymer and graphene oxide) have been used as adsorbents for the removal of As from water (Liu et al., 2020). Recently, biopolymers like chitosan has received much attention for the removal of As (Gupta et al., 2012). It is well known that the use of biopolymer for the removal does not guarantee an acceptable performance in case of arsenic ion removal. Therefore, it is anticipated that modifications and functionalization of the sorbents original structure could greatly enhance their affinity for the removal of arsenic.

Utilizing cross-linked, gel, and microsphere of chitosan are advanced techniques to enhance the stability, mechanical strength, and reusability of chitosan. Furthermore, embedded a metal like iron, molybdenum, etc. into chitosan microsphere is an effective way to boost the adsorption property of chitosan (Ayub et al., 2020; Boddu et al., 2008; Pontoni and Fabbricino, 2012). Interestingly, the incorporation of iron into the chitosan matrix to form iron-chitosan composite have been proposed for the removal of arsenic from water. Iron-chitosan flakes (ICSF) and iron-chitosan granules (ICSB) have been reported (Gupta et al., 2009). Under equilibrium and dynamic conditions, ICSF showed higher adsorption capacity for both As (III) and As(V) than ICSB, however, the column experiments demonstrated that ICSB have reduced arsenic concentration from 500 to  $< 10 \mu\text{g l}^{-1}$ . This promising technique was used to fabricate chitosan microspheres impregnated with iron (F-ICSM) for removing As(V) from an aqueous solution (Lobo et al., 2020). It has been found from studying the impact of the embedded concentration of Fe at 0.7, 5.5 and 11.2 g Fe<sup>3+</sup>/100 g of chitosan at pH range from 4 to 9 that the increase in Fe proportion is favorable at pH range from 6 to 9. Besides, the recyclability test clarified that the residual concentration of As(V), even after using F-ICSM for four cycles, was still lower than the acceptable by WHO (0.01 mg/L) in drinking water. Additionally, it has been noticed that there is no significant loss in F-ICSM, suggesting an excellent mechanical strength of the fabricated microspheres. Moreover, it was found that the adsorption of As(V) onto F-ICSM followed Langmuir isotherm model with a maximum adsorption capacity of 120.77 mg·g<sup>-1</sup>. Further, the incorporation of magnetic iron oxide into chitosan film greatly improved its adsorption capacity from 1.6 to 10.4 mg·g<sup>-1</sup>, accompanied with a rapid adsorption saturation in case of magnetic iron oxide chitosan film (Kloster et al., 2020). Similarly, Gogoi et al. (Kloster et al., 2020) reported the maximum adsorption capacity of As(V) onto for onto chitosan coated magnetite reached 10.8 mg·g<sup>-1</sup> (Wang et al., 2014).

Among studies that have been done on the adsorptive removal of As(III) in the last decade, using graphene oxide (GO)-modified chitosan is recognized as an efficient and cost-less adsorbent (Sherlala et al., 2019; Shan et al., 2020; Kumar and Jiang, 2016). Few investigations included utilizing CS/GO composite for the removal of As(III) ions, revealing the applicability of this composite for removing various heavy metals. Sherlala et al. (Sherlala et al., 2019) used chitosan-magnetic graphene oxide (CS/MGO) composite as an easily separable adsorbent for removing As(III) from an aqueous solution. CS/MGO composite showed the high surface area ( $S_{\text{BET}} = 152.38 \text{ m}^2/\text{g}$ ) and excellent magnetic property

( $M_s = 49.30 \text{ emu/g}$ ). It has been observed that the highest adsorption capacity and removal (%) of As(III) were 45 mg·g<sup>-1</sup> and 61%, respectively, at pH 7.3. Besides, the recyclability test confirmed the reusability of CS/MGO composite at which the removal (%) of As(III) slightly decreased after five consecutive adsorption/desorption cycles. In another attempt,  $\alpha$ -FeO(OH)/GO/CS nanocomposite was utilized to adsorb As(III) ions from an aqueous solution (Shan et al., 2020). The concrete results referred that the incorporation of  $\alpha$ -FeO(OH) into the adsorbent matrix significantly improved the adsorption capacity CS/GO composite towards As(III) reached 289.4 mg·g<sup>-1</sup>.

In one study, As(III) and As (V) were removed from wastewater using zeolite or clays chitosan-based adsorbents (Mukhopadhyay et al., 2019; Cho et al., 2012; Han et al., 2019). It was found that the increase in the amount of zeolite was accompanied by an increase in the flux, suggesting the increase in the membrane porosity that directly improves the hydrophilicity (Mukhopadhyay et al., 2019). These observations were in the agreement with the obtained SEM analysis for zeolite/chitosan membrane with different amounts of zeolite ranging from 0.25 to 1.25 wt%, to prove the increase in porosity going well with the increase in the amount of zeolite in adsorbent matrix. The best conditions for the adsorption of As (III) onto the as-fabricated membrane were observed to be at pH 6.3–8.3, with zeolite concentration ranged from 1.0 to 1.25 wt%. It was suggested that the As(V) adsorption onto CS-coated Na-X zeolite occurs via As–N and As–O bonding, and the surface hydroxyl group of Al–OH and –NH<sub>2</sub> were involved in the uptake As(V) from acid wastewater (Han et al., 2019). Furthermore, montmorillonite clay incorporated chitosan (MMT/CS) nanocomposite was fabricated by the gelation method for the removal of As(V). It was observed that MMT clay layers were well delaminated in between the polymer chains and the sorption. Therefore, a monolayer chemisorption took place, while the adsorption process was well-described by the pseudo-second order kinetic model with a maximum adsorption capacity of 3.4 mg·g<sup>-1</sup> (Cho et al., 2012). Moreover, Boddu et al. studied the adsorption aptitude of CS coated ceramic alumina to adsorb As(III) and As (V) ions. The maximum adsorption capacities of As (III) and As(V) ions reached 56.50 and 96.46 mg·g<sup>-1</sup> at pH 4, respectively, under equilibrium and dynamic conditions. Through column adsorption study, it was observed that there is no As in the effluent up to 40 bed volume for As(III) and 120 bed volume of As(V) ions (Boddu et al., 2008).

In another study, Wang and coauthors suggested that coating of chitosan biopolymer on the surface of Fe<sub>3</sub>O<sub>4</sub> nanoparticles significantly improved the adsorbability of magnetic chitosan/ZnO/alginate (MCS/ZnO@SA) gel beads toward As(V). The developed adsorbent beads (Fig. 3a) were formulated using mass ratio 1:1:1 for MCS:ZnO:SA via the coprecipitation technique, while Ca ions were used for the ionic crosslinking. The results indicated that As(V) ions could be adsorbed through chemical adsorption with a maximum adsorption capacity of 63.69 mg·g<sup>-1</sup> at pH 6. Moreover, it was observed that MCS/ZnO@SA beads showed the highest adsorption capacity (32.05 mg·g<sup>-1</sup>) as well as the highest removal percentage (98.99%) compared to CS, MCS and MCS/ZnO (Fig. 3b). The authors reported that Fe<sub>3</sub>O<sub>4</sub> has a significant adsorption aptitude towards As(V), since the MCS displayed better adsorption profile compared to neat CS. Besides, the formulated MCS/ZnO@SA composite beads

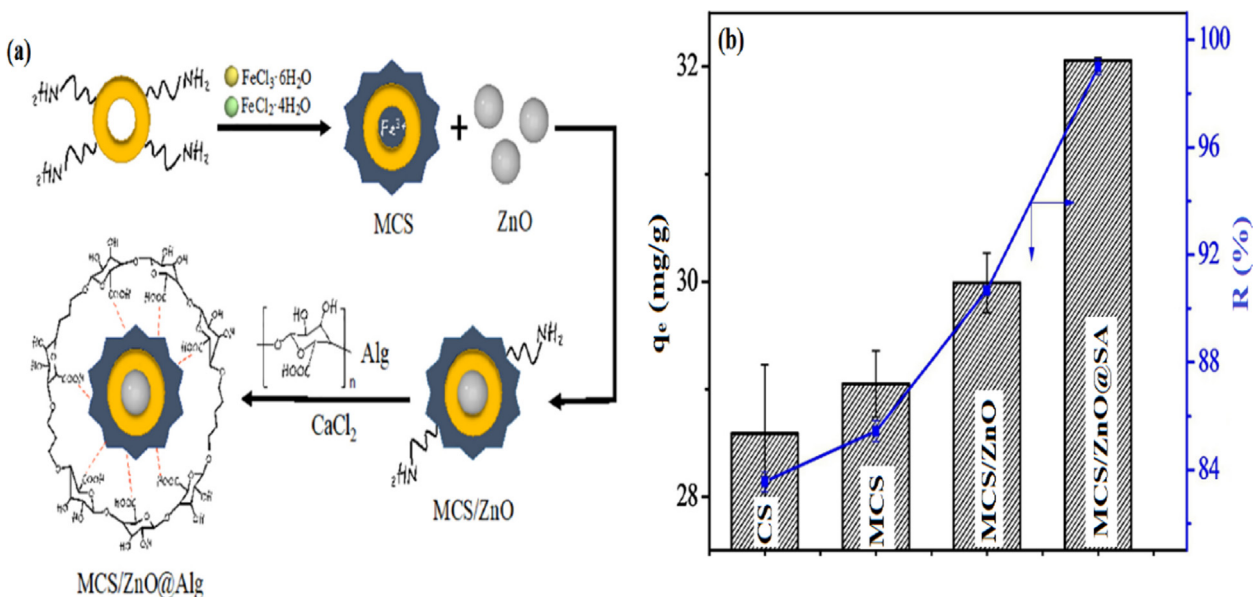


**Fig. 3** (a) A schematic diagram describes the preparation of MCS/ZnO@Alg beads, (b) adsorption profiles for CS, MCS, MCS/ZnO and MCS/ZnO@Alg beads toward As(V). Reprinted with permission from (Wang et al., 2019); Copyright 2021, Elsevier.

displayed acceptable recyclability with high adsorption performance (Wang et al., 2019).

### 3.2. Removal of copper

Copper (Cu(II)) ions can also contribute to water contamination with heavy metals. Cu(II) at a concentration below 0.05 ppm is an essential nutrient for living beings, according to regulations by WHO (Zhu et al., 2016). The accumulation of a higher concentration of Cu(II) in the human body affects the metal ions balance in the central nervous system, damages the liver as well as causes cancer by triggering some mutation (Saleem et al., 2020; Yang et al., 2021). Essentially, Cu(II) appears in water bodies from wastewater industries including mining, printing, dyes, electroplating and electrical combustion. Therefore, treatment of these industrial effluents has drawn great attentions of researchers (Hosseinzadeh and Ramin, 2018; Wang et al., 2020). Amongst the adsorbents that have evolved to efficiently remove Cu(II) from water bodies is chitosan.

In one attempt, He et al. studied the removal of Cu(II) by amidoxime-functionalized chitosan (AM/AO/AEBI-CS) (He et al., 2021). The adsorption capacity was deeply investigated as a function of pH solution, initial concentration, process temperature, and coexisting ions. The maximum adsorption capacity of Cu(II) onto AM/AO/AEBI-CS was 190.7 mg·g<sup>-1</sup>. Moreover, the presence of coexisting cations such as Na<sup>+</sup>, K<sup>+</sup>, or Ca<sup>2+</sup> merely interfered with the adsorption of Cu(II) onto AM/AO/AEBI-CS which may be attributed to the hydrated radii and electronegativity, resulting in a slightly decline in the adsorption profile of Cu(II).

In another attempt, Zhang et al. reported that stacking structure of chitosan membrane greatly enhanced the adsorption capability of chitosan towards Cu(II) ions in multilayer adsorption manner. The CS stacking membrane was constructed based on alternating electrospinning techniques. The

results obtained from this study referred that electrospinning technique significantly boosted the specific surface area of the as-fabricated chitosan stack membranes (18.7–25.1 m<sup>2</sup>·g<sup>-1</sup>), and consequently enriched the adsorption of the membrane towards Cu(II) ions. The adsorption capacity of Cu(II) was found to be increased with rising pH value from 2 to 6, while both of NH<sub>2</sub> and OH group partaken in the adsorption process. The adsorption reached equilibrium within 1 h, and a superior adsorption capacity has been attained with a maximum value of 276.2 mg·g<sup>-1</sup> (Zhang et al., 2019).

Recently, new efficient adsorbent beads were constructed by He et al. via grafting of ethylenediamine tetraacetic acid (EDTA) onto the surface of polyvinyl alcohol (PVA)-chitosan mixed beads. The developed beads showed substantially higher adsorption values compared to native chitosan beads. The maximum adsorption capacity of Cu(II) was 127.81 mg·g<sup>-1</sup>, with Langmuir isotherm model and the pseudo second order kinetic were well-describing the adsorption process. Also, the adsorbent beads persisted structurally-intact even at a strong acidic conditions (pH 2) (He et al., 2020). Furthermore, Sabourian et al. (Sabourian et al., 2016) reported another study on the fabrication of amine-functionalized chitosan for the removal of Cu(II) ions from aqueous media. It was found that the fabricated chitosan/tetraethylorthosilicate/aminopropyl triethoxysilane nanofibers (CS/TEOS/APTES) has an extra high adsorption capacity toward Cu(II) ions at which  $q_{max}$  reached 640.50 mg·g<sup>-1</sup> within 30 min at 45 °C. In addition, Fan and his coworkers (Fan et al., 2017) fabricated tetraethylenepentamine modified chitosan/CoFe<sub>2</sub>O<sub>4</sub> (TEPA/CS/CoFe<sub>2</sub>O<sub>4</sub>) composite for the adsorptive removal of Cu(II) ions from an aqueous solution. It was deduced from the comparative study between the TEPA/CS/CoFe<sub>2</sub>O<sub>4</sub> composite and other magnetic chitosan adsorbents that the as-fabricated composite possesses an excellent magnetic property, since the saturated magnetization (63.83 emu/g) is a benefit for the easy separation after completion of the

adsorption process. Furthermore, TEPA/CS/CoFe<sub>2</sub>O<sub>4</sub> composite revealed a fast separation at which the maximum adsorption capacity of Cu(II) was 168.06 mg·g<sup>-1</sup> at interval time around 10 min.

In another investigation, Zhang et al. (2019) focused on fabricating magnetic bentonite/carboxymethyl chitosan-/sodium alginate composite hydrogel beads (Mag-Ben/CCS/SA) for removing Cu(II) ions (Fig. 4a). Mag-Ben/CCS/SA were well characterized by various techniques to determine its structure and properties. It was found from the well-studied Cu(II) adsorption process that Mag-Ben/CCS/SA hydrogel beads provided a fast separation at which the Cu(II) removal efficiency reached 92.62% during 90 min at pH 5. Besides, the experimental data fitted pseudo-second order and Langmuir model with a maximum adsorption capacity reached 56.79 mg·g<sup>-1</sup>. Authors signified that the variation of pH medium greatly affected the adsorption of Cu(II), since the removal rate was found to be increased from 30.01 to 97.00% with increasing pH of the adsorption medium from 2.3 to 6.3 (Fig. 4b), indicating that the adsorption of Cu(II) by magnetic hydrogel beads is easier to accomplish at higher pH values. Moreover, the reusability test asserted the ability of Mag-Ben/CCS/SA hydrogel beads to recycle and reuse for

many cycles with high efficiency since the removal percent still over 85% after the fifth cycle as displayed in Fig. 4c.

In another study, chitosan-g-poly (acrylic acid) modified attapulgite (CS-g-PAA/APT) was utilized to remove Cu(II) ions from wastewater. The combination of APT clay with CS-g-PAA network provided an enhanced specific surface area and porous surface. Furthermore, the adsorption process of Cu(II) onto CS-g-PAA/APT was incredibly fast and over than 90% of the maximum adsorption capacity occurred during the initial 15 min (Wang et al., 2009). Moreover, Gandhi et al. (Gandhi and Meenakshi, 2012) evaluated the removal of Cu(II) by silica gel/chitosan composite (SiCS). A series of adsorption experiments were performed in batch mode to optimize the Cu(II) adsorption onto SiCS composite including pH, initial concentration, temperature, and interfering ions. The adsorption study displayed ultra-high adsorption capacity of Cu(II) onto SiCS composite ( $q_{\max} = 870 \text{ mg}\cdot\text{g}^{-1}$ ) at pH 5 with the composite dose of 100 mg at 30 °C. A slight decrease in the adsorption capacity of Cu(II) was noticed in the presence of interfering ions such as Ca<sup>2+</sup>, NO<sub>3</sub><sup>-</sup> and Cl<sup>-</sup>. While the impact of other interfering ions such as Mg<sup>2+</sup>, SO<sub>4</sub><sup>2-</sup> and HCO<sub>3</sub><sup>-</sup> could not be investigated as these ions form a precipitate with Cu(II).

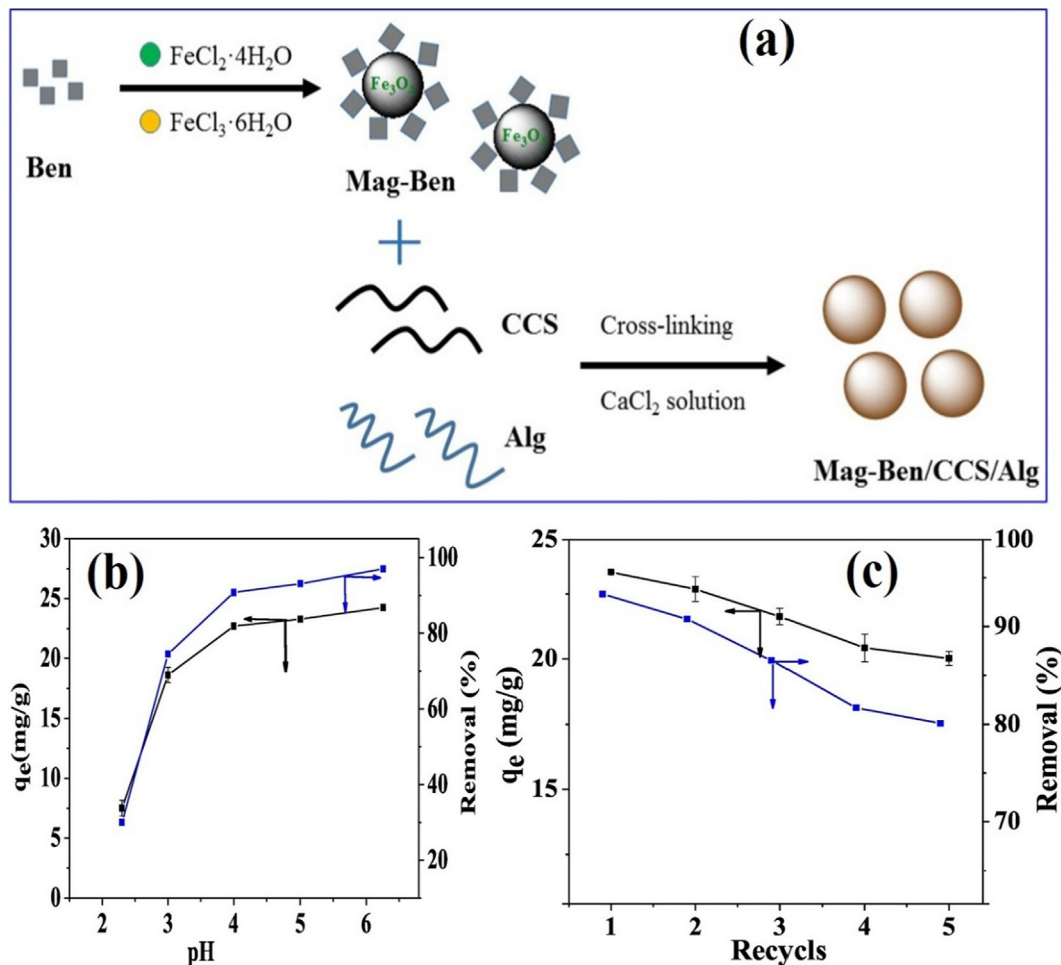


**Fig. 4** (a) a schematic diagram describes the preparation of Mag-Ben/CCS/Alg hydrogel beads, (b) effect of pH on the adsorption profile and (c) reusability profile for Mag-Ben/CCS/Alg hydrogel beads MCS/ZnO@Alg beads. Reprinted with permission from (Zhang et al., 2019); Copyright 2021, Elsevier.

Another study elucidated the impact of the presence of coexisting cations such as ( $\text{Na}^+$ ,  $\text{Ca}^{2+}$  and  $\text{Fe}^{3+}$ ) on the adsorption of  $\text{Cu}^{2+}$  ions onto chitosan grafted maleic acid composite (CS-g-MA). The results clarified that the existence of  $\text{Fe}^{3+}$  had great leverage on the efficacy of the adsorption process which may be due to the formation of hydroxyl-Fe coated CS-g-MA that intercalates  $\text{Cu}^{2+}$  ions. On the contrary,  $\text{Na}^+$  and  $\text{Ca}^{2+}$  caused a decrease in the  $\text{Cu}^{2+}$  adsorption capacity which may be attributed to the competition between  $\text{Cu}^{2+}$  and the interfering cations ( $\text{Na}^+$  and  $\text{Ca}^{2+}$ ) for the negative adsorption sites on the surface of CS-g-MA. Besides, the increase in the cations around the composite surface causes a shielding of  $\text{Cu}^{2+}$  that directly decreases the adsorption efficacy (Ibrahim et al., 2019).

Recently, Ionic liquids have meaningfully enhanced eco-friendly profits compared to the traditional materials. Ionic liquids (IL) have been used effectively for modification of neat chitosan as a novel green approach to ameliorate its adsorption aptitudes toward various pollutants (Liu et al., 2015; Wei et al., 2013). This is due to their exceptional properties including miscibility with organic solvents and water, non-toxicity, good thermal stability, minimal volatility and their abilities for recovery of metal ions from their aquatic systems. Cunha and co-workers examined the impact of ionic liquids on the copper adsorption profiles of functionalized chitosan beads (Cunha et al., 2019). Two different ionic liquids were used for the modification of pristine chitosan, namely 2-hydroxy ethylammonium formate (HEAF) and n-methyl 2-hydroxy ethylammonium butyrate (HEAB). The results clarified that IL functionalization endorses a significant improvement in the crystallinity, morphology and thermal stability of chitosan beads. At constant pH 5.5 and 298 K, the adsorption capacity was augmented after incorporation of IL into chitosan beads at lower Cu (II) concentrations ( $20 \text{ mg L}^{-1}$ ). The IL-functionalized chitosan offered a better correlation for the pseudo-second order kinetic model, confirming the chemisorption process, while the Isotherms data for Cu(II) ions adsorption were well-fitted to both Langmuir and Freundlich isotherm models. The results of refereed that the functionalization of chitosan by IL could be a promising strategy for fabrication of efficient adsorbents for Cu (II) ions removal.

Similarly, and authors have been used ionic liquid as a solvent for the fabrication of a novel magnetic cellulose-chitosan composite microsphere (NMCMs) by the sol-gel transition technique (Peng et al., 2014). The developed microspheres displayed porous structure, large specific surface area, and effec-tual Cu(II) uptake capacity. The adsorption quantity of Cu(II) enlarged sharply within the first 1.5 h, while maximum adsorption capacity was achieved after 20 h and recorded  $65.8 \text{ mg/g}$  at pH 5.0 using initial Cu(II) concentration of  $150 \text{ mg/L}$ . Furthermore, the presence of various coexisting ions has no observable influence on the Cu(II) adsorption on to NMCMs. Besides, the formulated microspheres displayed better reusability for five consecutive cycles without any loss in the adsorption characteristics.

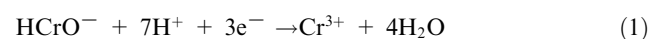
### 3.3. Removal of chromium

The excessive usage of chromium observed recently in diverse industries, including electroplating, textile dyeing, mining, leather tanning, steel and automobile manufacturing, creating

an additional heavy metal contamination in wastewater with increasing its potential hazard (Wei et al., 2019; Cao et al., 2021). Chromium naturally exists in two common oxidation states; Cr(III) and Cr(VI), while Cr(VI) more threatening human health as well as plant and animal than Cr(III). Furthermore, Cr(VI) is classified by International Agency for Research in cancer in group 1 (carcinogenic to humans) while Cr (III) in group 3 (not carcinogenic) (Dehghani et al., 2016; Cai et al., 2019). Consequently, the reduction of Cr(VI) to Cr(III) is considered as a critical to minimize its toxicity (Li et al., 2017).

In aqueous solutions, pH of the adsorption medium has a direct impact on the form of Cr. Cr(VI) exists as  $\text{H}_2\text{CrO}_4$  at pH 1, while it exists as  $\text{Cr}_2\text{O}_7^{2-}$  and  $\text{HCrO}_4^-$  at pH ranging from 2 to 6 and  $\text{CrO}_4^{2-}$  is the prime form at pH > 6 (Omer et al., 2019; Yi et al., 2020). Therefore, the existence of Cr(VI) in a neutral form ( $\text{H}_2\text{CrO}_4$ ) at pH 1 leads to a decrease in the columbic interaction between the positively charged amino groups in chitosan and the neutral  $\text{H}_2\text{CrO}_4$  molecules. At pH 2, the protonation of  $\text{NH}_2$  groups of chitosan occurs, resulting more surface positive charges. Consequently, the electrostatic attraction forces between the positively charged  $\text{NH}_3^+$  groups and the negatively charged Cr(VI) ions increased, leading to an improvement in the adsorption manner. On contrary, beyond pH 2 there is a significant decrease in the protonation of  $\text{NH}_2$  groups accompanied with a decrease in the positive charges on chitosan surface. Accordingly, the columbic interaction between chitosan and Cr(VI) decreases (Vieira et al., 2018; Wan et al., 2018).

In this regard, Omer et al. scrutinized the adsorption property of aminated chitosan (AmCS)-modified metal-organic framework towards the adsorptive removal of Cr(VI) (Omer et al., 2021). It was found that introducing extra amine groups to neat chitosan biopolymer boosted its cationic nature which is beneficial for adsorption of anionic Cr(VI) via electrostatic attractions. Furthermore, AmCS was further modified by ZIF-67 for enhancing the surface area and the adsorption capacity of chitosan. While  $\text{Fe}_3\text{O}_4$  was used for facilitating the beads separation after completion of the adsorption process SEM analysis in addition to cross-sectional stereo microscope of the developed  $\text{Fe}_3\text{O}_4/\text{ZIF-67@AmCS}$  composite beads displayed cores that surrounded by double shells, proving the formation of core-dual shell structure (Fig. 5a, b). The adsorption study signified that the removal of Cr (VI) ions was greatly improved compared to native AmCS, ZIF-67 and  $\text{Fe}_3\text{O}_4$ . In addition, the removal percent gradually increased with increasing AmCS ratio in the composite beads (Fig. 5c). Moreover, the calculated  $q_{\max}$  was found to be  $119.05 \text{ mg.g}^{-1}$  at pH 2. Besides, the authors observed that coexisting anions  $\text{Cl}^-$  and  $\text{NO}_3^-$  slightly decreased the adsorption capacity compared to  $\text{SO}_4^{2-}$  anions as a result of low-affinity ligands in case of  $\text{Cl}^-$  and  $\text{NO}_3^-$  anions which form weak outer-sphere complexes with the beads surface. While,  $\text{SO}_4^{2-}$  anions have strong-affinity ligands which able to form both of inner and outer sphere composites that reduces some of the adsorption sites, and consequently declines the adsorption capacity (Fig. 5d). It was suggested that the adsorption mechanism of Cr(VI) ions onto the composite beads occurred via the reduction of Cr(VI) to Cr(III) as summarized in the following equations (Omer et al., 2021):



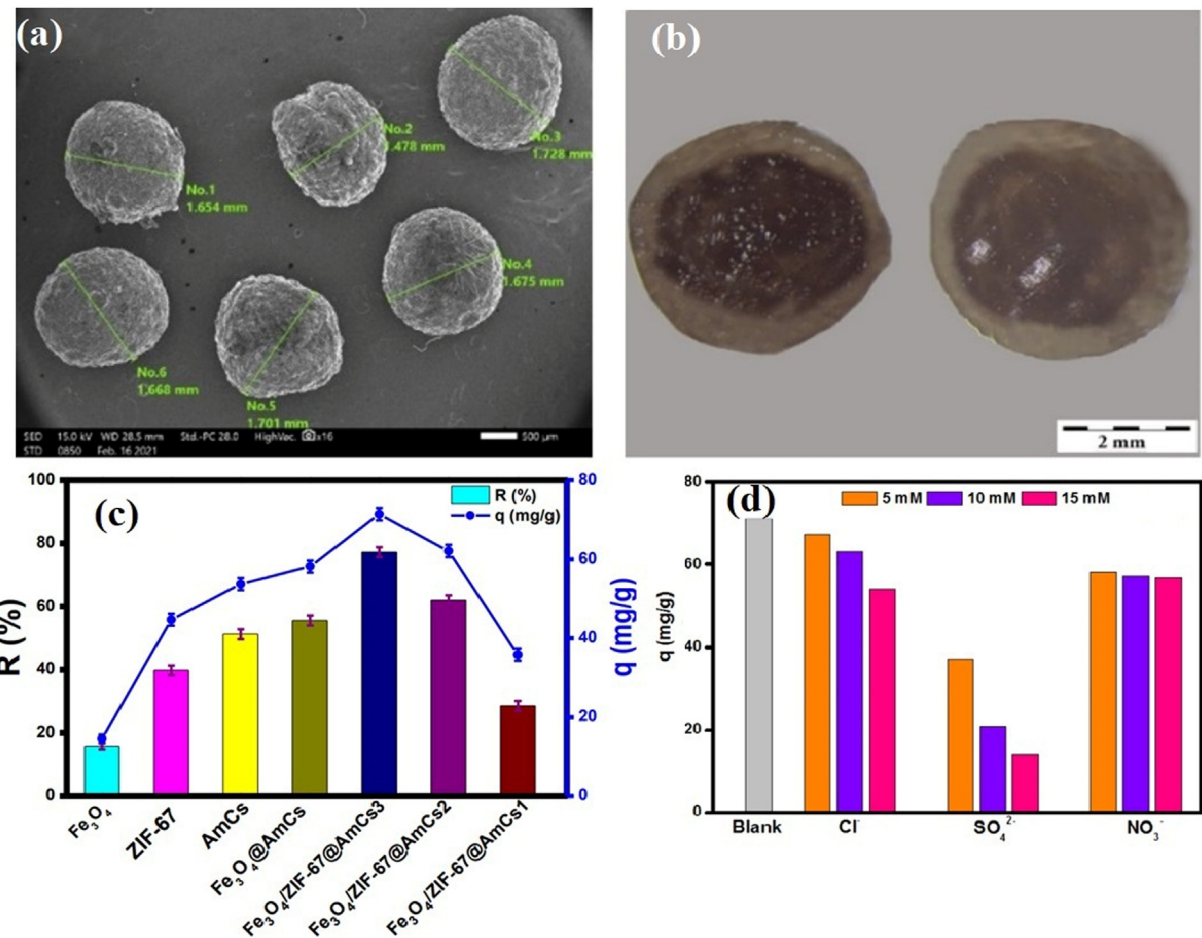
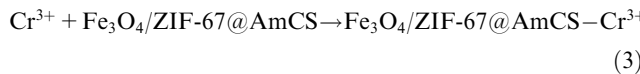


**Fig. 5** (a) SEM image of Fe<sub>3</sub>O<sub>4</sub>/ZIF-67@AmCS composite beads (b) cross-sectional stereo microscope of Fe<sub>3</sub>O<sub>4</sub>/ZIF-67@AmCS composite beads, (c) Adsorption profiles of AmCS, ZIF-67 Fe<sub>3</sub>O<sub>4</sub> and Fe<sub>3</sub>O<sub>4</sub>/ZIF-67@AmCS composite beads and (d) Effect of coexisting anions on the removal of Cr(VI). Reprinted with permission from (Omer et al., 2021); Copyright 2021, Elsevier.



In another study, Eltaweil et al. (2021) developed fast and reusable adsorbent (ATP@Fe<sub>3</sub>O<sub>4</sub>-AmCS composite) based on the modification of AmCS with attapulgite clay and magnetic Fe<sub>3</sub>O<sub>4</sub> nanoparticles for the adsorptive removal of anionic Cr(VI). It was noticed that the adsorption process seems to be efficient and fast, since the maximum adsorption capacity of Cr(VI) reached 294.12 mg·g<sup>-1</sup> within 60 min. Moreover, recyclability test inferred the mechanical stability at which the Cr(VI) adsorption capacity was 62.54 mg·g<sup>-1</sup> after ten cycles. Besides, it was proposed that the adsorption mechanism of Cr(VI) onto ATP@Fe<sub>3</sub>O<sub>4</sub>-NH<sub>2</sub>CS composite include electrostatic interactions between the positively protonated NH<sub>3</sub><sup>+</sup> on adsorbent surface and the negatively charged Cr(VI) anions, reduction of Cr(VI) to Cr(III) and ion-exchange process as clarified in Fig. 6.

From the economical point of view, choosing an adsorbent for the practical application depends on strict criteria including its efficiency, reusability, stability and it should provide a fast adsorption process. Indeed, there are numerous efficient, reu-

sable and stable adsorbents, but the fourth condition is not usually provided in most adsorbents. Therefore, several studies have worked on this flaw to fulfill a perfect adsorbent. For this purpose, Dinh et al. (2020), reported a fast adsorption process of Cr(VI) onto the as-fabricated MnO<sub>2</sub>/CS nanocomposite. It was observed during ongoing study of the predominant factors on the Cr(VI) adsorption that the removal efficiency of Cr(VI) reached 92% within 60 min at pH 2. Moreover, the isotherms study deduced that the adsorption of Cr(VI) onto MnO<sub>2</sub>/CS nanocomposite included the monolayer and multilayer adsorption depending on the concentration of Cr(VI). While the kinetics study suggested that the Cr(VI) adsorption onto MnO<sub>2</sub>/CS was a physical process which could be due to the electrostatic attraction between the anionic Cr(VI) and positively charged sites MnO<sub>2</sub>/CS nanocomposite.

In this context, Shen et al. (Shen et al., 2013) reported an efficient and fast adsorptive removal of Cr(VI) onto the as-fabricated chitosan-Fe(III) complex. It was found that the maximum adsorption capacity of Cr(VI) onto the complex was 173.1 mg·g<sup>-1</sup> in 10 min. Furthermore, it was hypothesized that the adsorption mechanism of Cr(VI) onto chitosan-Fe(III) complex occurred via partial reduction of Cr(VI) to Cr(III), with monitored evidences of electrostatic interaction between the amine groups onto the surface of chitosan and

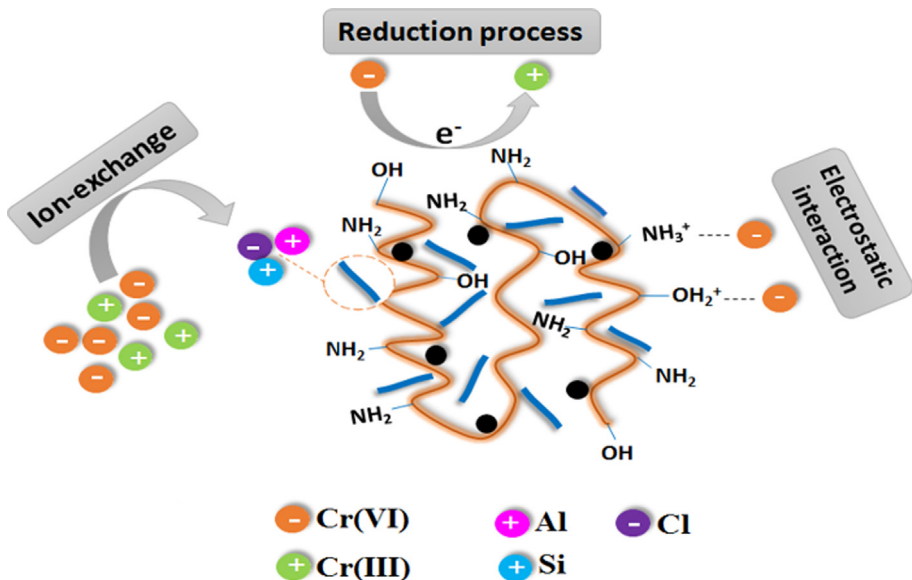


**Fig. 6** The suggested mechanism for the adsorption of Cr (VI) on ATP@Fe<sub>3</sub>O<sub>4</sub>-AmCS magnetic composite. Reprinted with permission from (Eltaweil et al., 2021); Copyright 2021, Springer Nature.

the anionic Cr(VI). Another study recommended triethylenetetramine-modified hollow Fe<sub>3</sub>O<sub>4</sub>/SiO<sub>2</sub>/chitosan magnetic nanocomposite (Fe<sub>3</sub>O<sub>4</sub>/SiO<sub>2</sub>/CS-TETA) to be an efficient adsorbent for removing Cr(VI) ions. Fe<sub>3</sub>O<sub>4</sub>/SiO<sub>2</sub>/CS-TETA composite possesses many adsorption sites for Cr (VI), resulting in high  $q_{\text{max}}$  reached 254.6 mg·g<sup>-1</sup> during 15 min (Wang et al., 2020).

In yet another attempt, Chen et al. (2013) investigated the utilization of chitosan/montmorillonite magnetic microspheres (CS/xMMT–Fe<sub>3</sub>O<sub>4</sub>) as an efficient adsorbent for removing Cr (VI) ions. The key parameters of the Cr(VI) adsorption process were adequately evaluated including solution pH, CS/xMMT–Fe<sub>3</sub>O<sub>4</sub> microspheres dose, Cr(VI) initial concentration, system temperature and MMT proportion. The results clarified that the equilibrium adsorption capacity of Cr(VI) onto CS/xMMT–Fe<sub>3</sub>O<sub>4</sub> microspheres directly decreased from 58.82 to 35.71 mg·g<sup>-1</sup> with the increase in MMT proportion from 10 to 110 wt%. This behavior was explained by the decrease in the amount of NH<sub>2</sub> groups, the main responsible for the Cr (VI) adsorption process on the microspheres with the increase in MMT proportion. Furthermore, the highest adsorption capacity of Cr(VI) onto the microsphere occurred at a low acidic medium (pH 2) and high temperature (60 °C). In another study highlighting fabrication of an easily separable chitosan composite with a developed adsorption capacity towards Cr(VI) ions. Moreover, the as-fabricated Fe<sub>3</sub>O<sub>4</sub>-chitosan@bentonite composite (Fe<sub>3</sub>O<sub>4</sub>-CS@Ben) possesses a good magnetic property, high stability and good adsorption capacity towards Cr(VI) in the aqueous solutions with  $q_{\text{max}}$  to be 62.1 mg·g<sup>-1</sup> and the removal efficiency decreased only 3% after five sequential cycles (Rios et al., 2008).

Another type of chitosan-based adsorbent in form of hydrogel has been developed by Vilela, et al. The adsorbent hydrogel was synthesized using chemical crosslinking of chitosan with poly (acrylic acid) in the presence of N,N'-methylene bisacrylamide as a crosslinker. The results obtained from this study signified that adsorption of Cr (VI) increased with

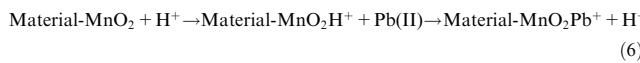
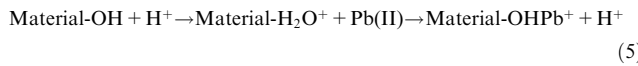
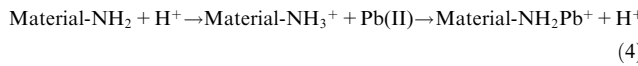
decreasing pH as a result of the generated changes in the ionic network of adsorbent hydrogel. Moreover, the maximum removal (%) was achieved at pH 4.5 using 100 mg·g<sup>-1</sup> of initial chromium ions concentration and recorded 94.72%, while the maximum adsorption capacity was found to be 93.03 mg·g<sup>-1</sup> (Vilela et al., 2019).

### 3.4. Removal of Lead

Lead (Pb(II)) is one of the most persistent heavy metals that menace humans and the ecosystem when its concentration in potable water exceeds the tolerance limit that is authorized by WHO to be 10 ppb (Dong et al., 2019; Chen et al., 2020). According to US Environmental Protection Agency (EPA), the overall Pb(II) concentration allowance in the drinking water is 15 ppb (Saleh et al., 2019; Wang et al., 2020). Piling up of Pb(II) in the human body damages liver, central nervous system, kidney and decreases hemoglobin formation (Sani et al., 2017). Therefore, various state-of-the-art techniques have been developed to overcome this deadly jeopardy including ion exchange, adsorption, membrane filtration, and precipitation (Geisse et al., 2020). There are several studies recommended adsorption as the best technique to remove Pb (II) from wastewater, without producing secondary pollutants, as well as the possibility to recycle the used adsorbent for many times with high efficiency (Gao et al., 2021). Many studies have been carried out to develop adsorbents that have the propensity to be recycled and reuses, such as chitosan and its derivatives. In this context, Gao et al. developed a new alginate/melamine/chitosan (SA/ME/CS) aerogel for the adsorptive removal of Pb(II) ions. A series of adsorption experiments were carried out in batch mode to find out the best conditions to adsorb Pb(II) onto SA/ME/CS aerogel. Besides, it was noticed that SA/ME/CS aerogel still had a high affinity towards the adsorption of Pb(II) in the existence of the coexisting divalent metals such as Co(II), Ni(II), Cd(II) and Cu (II). The promising results asserted that SA/ME/CS aerogel

exhibited super high adsorption capacity towards Pb(II) at pH 5.5 with  $q_{\max}$  to be  $1331.60 \text{ mg}\cdot\text{g}^{-1}$ .

In one attempt, Dinh and coworkers (Dinh et al., 2018) suggested that the adsorption of Pb(II) onto the as-fabricated chitosan loaded  $\text{MnO}_2$  ( $\text{MnO}_2/\text{CS}$ ) nanoparticles occurred via the physical adsorption mechanism at which the surface of  $\text{MnO}_2/\text{CS}$  possesses various adsorption sites; with group such OH,  $\text{NH}_2$  and  $\text{MnO}_2$  to adsorb Pb(II) ions as represented in the following equations:



The ions-holes mechanism based on the theory that the size of the distributed pores on the surface of  $\text{MnO}_2/\text{CS}$  beads are much larger than the average radius of Pb(II) ions, suggesting the possibility of entering Pb(II) ions insides the holes of the beads. In another study, Guo et al. (Guo et al., 2018), examined utilizing CS-PDA aerogel for the adsorptive removal of Pb(II) from wastewater. The dominant factors on the Pb(II) adsorption process were studied, as well as the recyclability of the fabricated aerogel was assessed also. It was found that the  $q_{\max}$  of Pb(II) onto CS-PDA aerogel was  $441.20 \text{ mg}\cdot\text{g}^{-1}$  at pH 5.5. The reported results referred that the chemisorption process took place, while the adsorption mechanism of Pb(II) onto CS-PDA aerogel occurred via coordination bonds between Pb(II) ions and nitrogen atoms. Moreover, the recyclability test showed that CS-PDA aerogel can be an economical adsorbent as the adsorption capacity Pb(II) onto the aerogel was still  $> 80\%$  after eight cycles.

Cui and co-workers have been developed a rational approach using ionic liquids to enhance the adsorption competences of chitosan for the removal of Pb(II) as well as to avoid the agglomeration of chitosan-based adsorbent (Cui et al., 2013). The modification strategy was performed via the ion-ion interactions between carboxymethyl chitosan (CMCTS) as anion and Triethylmethyl ammonium chloride (Aliquat 336) as cation  $[\text{A336}]^+$  which acts as a self-ionic liquid (Fig. 7). The as-fabricated  $[\text{A336}][\text{CMCTS}]$  have both carboxyl and quaternary ammonium groups which offer admirable adsorption aptitudes for Pb(II) ions in real waste water, since the removal efficiency of Pb(II) reached 97.71% with a maximum adsorption capacity of  $143.3 \text{ mg g}^{-1}$ . In addition, a sharp increase in adsorption capacity value was achieved with rising pH from 2.0 to 3.5, followed by a slight increase at pH 4.4 and finally reached a plateau. The regeneration studies signified that about 90% of Pb (II) was desorbed using an eluting medium composed of  $0.1 \text{ mol L}^{-1}$  of EDTA solution and  $0.1 \text{ mol L}^{-1}$  DTPA solution. The gained results empathized that  $[\text{A336}][\text{CMCTS}]$  could be apply for the Pb (II) removal from wastewater derived from the rare earth industries.

In another study, Li et al. (Li et al., 2013) inspected the adsorptive removal of Pb(II) onto ethylenediamine-modified yeast biomass coated with magnetic chitosan microparticles (EYMCs) in batch system. The higher adsorption capacity of Pb(II) was achieved at pH range of 4–6. Furthermore, the equilibrium data were matched with Langmuir model and the calculated  $q_{\max}$  was found to be 121.26, 127.37 and  $134.90 \text{ mg}\cdot\text{g}^{-1}$  at 20, 30 and 40 °C, respectively. The desorption study illustrated the potential recovery of the fabricated EYMCs microparticles at which insignificant decrease in the adsorption capacity of  $0.61 \text{ mg}\cdot\text{g}^{-1}$  of Pb(II) onto EYMCs microparticles after the fourth cycle. Also, chitosan-poly vinyl alcohol (CS-PVA) nanofibers were successfully applied for

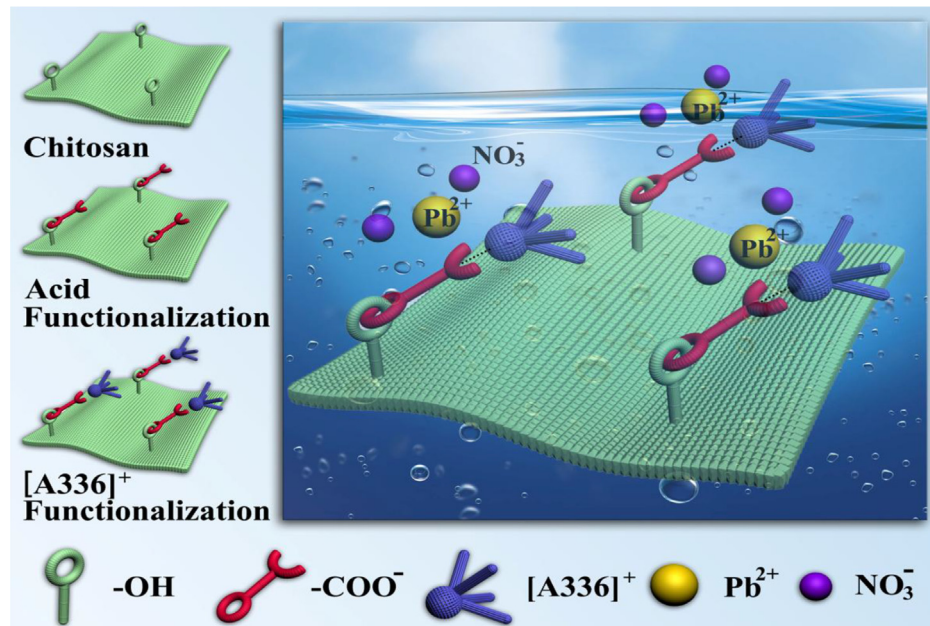


**Fig. 7** Schematic representation of the fabrication of  $[\text{A336}][\text{CMCTS}]$  adsorbent with various functional groups for adsorption of Pb(II) ions (Cui et al., 2013); Copyright 2021, Elsevier.

removing Pb(II) ions. The results pointed out that CS-PVA nanofibers possess high adsorption capacity toward Pb(II) ions with  $q_{\text{max}}$  to be  $266.12 \text{ mg}\cdot\text{g}^{-1}$  (Karim et al., 2019). Chitosan-zeolite nanocomposite is another variation to improve the adsorption property of chitosan from  $24.45$  to  $454.5 \text{ mg}\cdot\text{g}^{-1}$  with high removal efficiency of chitosan-zeolite nanocomposite even after fifth adsorption/desorption cycles, reflecting the high renewability of the as-fabricated composite (Shariatinia and Bagherpour, 2018).

Recently, Liang et al. focused on developing a new chitosan-based adsorbent with higher efficiency for the removal of Pb(II) ions (Liang et al., 2018). Solidified beads composed of synthesized metal organic framework MIL-125 and chitosan were fabricated via a template-free solvothermal method, while sodium tripolyphosphate (Na-TPP) was used as ionic cross-linker. The synthesized MIL-125-CS beads structure simplified the separation from water after completion of the adsorption process. The adsorption results clarified that 180 min were needed for the beads to reach equilibrium with a maximum adsorption capacity of  $406.5 \text{ mg}\cdot\text{g}^{-1}$  at room temperature. The maximum adsorption capacity of Pb(II) ions was sharply increased from  $40.1$  to  $101.75 \text{ mg}\cdot\text{g}^{-1}$  with increasing the pH from 2 to 6. However, further increase in pH value from 6 to 7 caused the adsorption profile dropped sharply. This finding was consistent with Ayati et al. study at which the higher Pb(II) removal efficiency was achieved at higher pH. In the presence of a high  $\text{H}^+$ , the adsorption sites of the adsorbent protonated. So, the adsorption competition between Pb(II) ions and  $\text{H}^+$  ions strongly increased, resulting in the adsorption of  $\text{H}^+$  hindered the specific adsorption of Pb(II) (Ayati et al., 2017). Furthermore, MIL-125-CS beads showed better adsorption performance with retain about 85% of its removal efficiency after reuse for five consecutive cycles of adsorption-desorption processes.

The same research group tried to improve the adsorption capacity as well as to boost the limited surface area of native chitosan through combination with ATP clay. The authors firstly combined ATP with  $\text{Fe}_3\text{O}_4$  to form  $\text{Fe}_3\text{O}_4/\text{ATP}$  (MATP) nanoparticles to overcome the difficult separation of ATP from the adsorption medium. Next, authors were modified  $\text{Fe}_3\text{O}_4/\text{ATP}$  with aminopropyltriethoxysilane (APTS) as a coupling agent before imbedding into CS gel beads to form APTS- $\text{Fe}_3\text{O}_4/\text{ATP}@\text{CS}$  composite beads. The obtained results elucidated that the adsorption profile of Pb(II) ions was augmented with a maximum adsorption capacity of  $625.34 \text{ mg}\cdot\text{g}^{-1}$  at the optimum pH 6. The developed beads demonstrated a large specific surface and adequate hardness, which was successfully reused for the adsorption of Pb(II) up to five cycles, while the removal rate continued higher than 84.8%. The adsorption process followed the pseudo-second order kinetic and Langmuir adsorption isotherm model (Liang et al., 2019).

In one investigation, Xu et al. deduced that the optimum pH of the adsorption of Pb(II) onto novel cross-linked carboxylated chitosan/carboxylated nanocellulose (CYCS/CNC) beads (Fig. 8a) (Xu et al., 2021). Furthermore, the wet CYCS/CNC beads were in perfect spherical shape, while the drying conditions produced collapsed and non-spherical beads as depicted in Fig. 8b, c. This in turn leads to increasing the surface charges of the CYCS/CNC beads (Fig. 8d), which consequently induce more of the electrostatic attractions between the negatively charged  $\text{COO}^-$  and the positively charged Pb

(II) cations, resulting an increase in the adsorption capacity ( $334.92 \text{ mg}\cdot\text{g}^{-1}$ ). Moreover, it was found the higher adsorption capacity of  $\text{Pb}^{2+}$  obtained at pH 5 which is most likely due to the ionization of the present  $-\text{COOH}$  groups on the adsorbent matrix. While at pH 2, the adsorption of Pb(II) was extremely low due to the weak electrostatic interactions between adsorbent and adsorbate, since the binding sites were mainly inhibited by the competition of the positively charged Pb(II) and  $\text{H}^+$  ions as presented in Eqs. (7) and (8). The possible mechanism for the adsorption of Pb(II) onto CYCS/CNC beads was mainly dependent on electrostatic interactions between Pb(II) and the active sites (viz.,  $-\text{OH}^-$  and  $-\text{NH}_2$ ) on the CYCS/CNC beads surface as clarified in Fig. 8c.



In an attempt, Hu et al. fabricated an easy separable adsorbent via incorporation of magnetic nanoparticles chitosan grafted polyacrylic acid (MCS-PAA) hydrogel for the removal of  $\text{Pb}^{2+}$  ions (Hu et al., 2020). The developed adsorbent displayed superior adsorption performance over the pure chitosan. The results clarified the maximum adsorption capacity of  $\text{Pb}^{2+}$  reached  $204.89 \text{ mg}\cdot\text{g}^{-1}$  within 50 min. The suggested adsorption mechanism was explained on the basis of the complexation occurred between Pb(II) and the presence of COOH,  $\text{NH}_2$  and OH groups in MCS-PAA hydrogel matrix. Additionally, it was observed that grafting of PAA on chitosan backbone clearly improved the acid-resistance of chitosan in regeneration studies, implying the excellent adsorption potential of the developed adsorbent. The reusability test elucidated a slight diminution in the adsorption capacity of  $\text{Pb}^{2+}$  after the 5th cycle at which the adsorption capacity of  $\text{Pb}^{2+}$  onto MCS-PAA was 58.97 and  $80.6 \text{ mg/g}$  using the eluents HCl and NaOH, respectively. Also, Tanhaei et al. inferred the renewability of the magnetic chitosan nanocomposite (EDTA-PCSF) since the amount of the adsorbed  $\text{Pb}^{2+}$  onto EDTA-PCSF decreased by 3.25% after the 4th cycle using HCl (Tanhaei et al., 2017).

### 3.5. Removal of cadmium

Cadmium (Cd(II)) has been classified as an extremely toxic metal because of its carcinogenic and teratogenic impacts (Pyrzynska, 2019). Cadmium is mainly drained into environment as a result of industrial effluents, mining operations, coal and oil combustion, and waste incineration. Accumulation of cadmium in environment is a serious problem, so the maximum allowed limit of cadmium in the drinking water is 0.003–0.005 ppm according to EPA and WHO (Godt et al., 2006). Based on the limited available amount of water and the high contamination of cadmium, the need of removal of these perilous contaminants from wastewater is crucial. Among the widespread adsorbents available for cadmium removal, chitosan based composite and hydrogels have gained great interest (Huang et al., 2017). In this regard, Babakhani et al. (Babakhani and Sartaj, 2020) reported a cost-effective technique for removing Cd(II) from wastewater by an environmentally benign adsorbent. Sodium tripolyphosphate cross-linked chitosan beads (STPP-CLCS) were synthesized at different concentrations of sodium tripolyphosphate; 5, 10, and

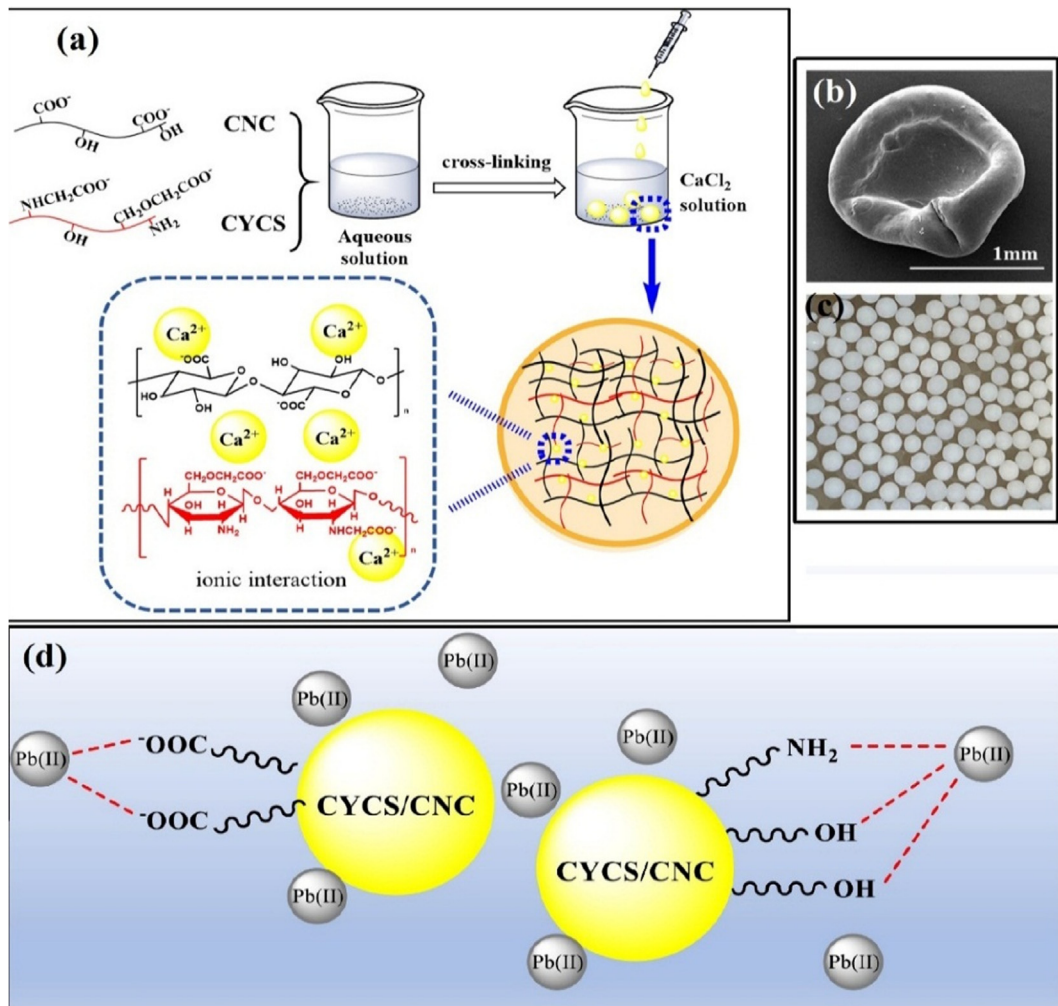


**Fig. 8** (a) Schematic representation of the preparation of CYCS/CNC beads, (b, c) SEM image and digital laboratory image for CYCS/CNC beads, respectively, (d) Effect of pH on the adsorption capacity and surface charges and (e) suggested mechanism for the adsorption of  $\text{Pb}(\text{II})$  on CYCS/CNC beads. Reprinted with permission from (Xu et al., 2021); Copyright 2021, Elsevier.

15% (w/v) to assess the impact of the crosslinking degree on the adsorption behavior of the cross-linked chitosan. Furthermore, to obtain higher adsorption capacity of  $\text{Cd}(\text{II})$  onto STPP-CLCS beads, the crucial parameters that affect the process efficiency were thoroughly investigated. The experimental results clarified that at low initial concentration of  $\text{Cd}(\text{II})$  the lower cross-linked chitosan beads revealed higher adsorption capacity. Consequently, the higher cross-linked chitosan had higher adsorption capacity at the high  $\text{Cd}(\text{II})$  concentration. Furthermore, the adsorption data were best modeled by Langmuir model, while the  $q_{\max}$  was  $99.87 \text{ mg}\cdot\text{g}^{-1}$  at  $55^\circ\text{C}$ , pH 7 and 2.92% (w/v) crosslinking degree. Besides, thermodynamic study indicated the feasibility of the random endothermic adsorption process. Moreover, sodium dodecyl sulfate surfactant-modified chitosan beads of diameter equal  $3.7 \pm 0.32 \text{ mm}$  with water content 97–98% were fabricated by Pal et al. to remove  $\text{Cd}(\text{II})$  ions from an aqueous medium (Pal and Pal, 2019). The surfactant-modified chitosan beads showed enhanced adsorption capacity of  $125.0 \text{ mg}\cdot\text{g}^{-1}$  with pseudo-second order model and Langmuir model better fitting. In another study, Vilela et al. (2019), evaluated the adsorption efficacy of chitosan-based hydrogel towards the removal of

$\text{Cd}(\text{II})$  from an aqueous media. It was found the  $\text{Cd}(\text{II})$  adsorption onto chitosan-based hydrogel with the optimum condition to achieve higher adsorption capacity was at pH 6 and  $40^\circ\text{C}$  using 100 mg chitosan-based hydrogel. Redlich-Peterson was the more suitable isotherm model to describe the equilibrium data, whereas pseudo-second order was the best fitted kinetic model. Moreover, the calculated  $q_{\max}$  according to Langmuir model was  $234.84 \text{ mg}\cdot\text{g}^{-1}$ . Besides, the desorption study indicated the formation of reversible chemical bonds between  $\text{Cd}(\text{II})$  and the active sites of the chitosan-based hydrogel. Due to their low cost, biodegradability, highly efficiency and biocompatibility, biocomposites based on chitosan and clay minerals have attracted much attention in the removal of heavy metal including cadmium. Chen et al. (2018) synthesized chitosan/vermiculite (CS-VMT) composite using epichlorohydrin to remove  $\text{Cd}(\text{II})$  from aqueous solutions. Results revealed that chitosan cannot intercalate into vermiculite interlayer space but cross linked on its external surface. The maximum adsorption capacity of CS-VMT composite for  $\text{Cd}(\text{II})$  was  $58.48 \text{ mg g}^{-1}$  at pH 4 with a good reusability (>90%) after four cycles. Experimental data fitted well pseudo-second-order and Langmuir

isotherm models. The main adsorption mechanism for the adsorption of Cd(II) onto CS-VMT was chelation along with electrostatic attraction. However, Quiroga et al. (Quiroga-Flores et al., 2019) developed a new recyclable silicate-titanate nanotubes embedded into chitosan (STNTs-CS) hydrogel for Cd(II) removal with enhanced adsorption capacity. Their results clarified that the kinetic rate of silicate-titanate nanotubes increased 3-times and that the diffusion rate increased 2-times prior to the embedment. Furthermore, the maximum adsorption capacity of the developed STNTs-CS hydrogel increased to  $656 \pm 27 \text{ mg}\cdot\text{g}^{-1}$  which is 2.3 times higher than the pristine STNTs.

In another attempt, Chen et al. (Chen et al., 2012) developed a novel type of chitosan composite which is thiourea-modified magnetic ion-imprinted chitosan/TiO<sub>2</sub> (MICST) for efficient removal of Cd(II) ions from wastewater. The obtained results pointed out that the apt pH for the perfect adsorptive removal of Cd(II) ions onto the as-fabricated MICST composite was found to be in the range 6–7. Furthermore, the kinetics study illustrated that experimental data could be represented by pseudo-second order. While the isotherms study demonstrated that Langmuir was the best isotherm model to describe the equilibrium data of the Cd(II) adsorption process onto MICST composite. It was found that the calculated  $q_{\max}$  under Langmuir model was  $256.41 \text{ mg}\cdot\text{g}^{-1}$ . The desorption study revealed that the adsorption capacity of Cd(II) onto the reused MICST composite was barely decreased after the fifth cycle. Also, Wang et al. (2020) prepared a novel, non-toxic and low cost shell-coated cobalt ferrite@SiO<sub>2</sub>-chitosan/EDTA composite with high adsorption capacity and outstanding recyclability using solvothermal and sol-gel process for the removal of Cd from contaminated water. The magnetic attapulgite was modified with EDTA and chitosan to utilize both carboxyl groups and amino groups along with nontoxic crosslinker STPP. The shell-coated cobalt ferrite@SiO<sub>2</sub>-chitosan/EDTA composite exhibited paramagnetic behavior. The maximum adsorption capacity of the prepared composite was up to  $127.79 \text{ mg}\cdot\text{g}^{-1}$  with removal efficiency up to 88% after the fifth cycle. Additionally, the shell-coated

cobalt ferrite@SiO<sub>2</sub>-chitosan/EDTA composite exhibited high selectivity in high ionic concentration experiments. It was recorded that the higher removal efficiency was at pH 7, agreeing with Karimi et al. study (Karimi et al., 2022). Upon strong acidic conditions, removal efficiency was fairly low, owing to the high concentration of H<sup>+</sup> ions, competing with Cd<sup>2+</sup> for the adsorption sites as well as the strong coulombic repulsion among protonated NH<sub>2</sub> of CS and Cd<sup>2+</sup>. Another easy separable magnetic chitosan composite (CS@nZVI) for the adsorptive removal Cd(II) was prepared by Ahmadi et al. (Ahmadi et al., 2017). Experimental results for the removal of Cd(II) onto CS@nZVI were fitted pseudo-second order and Freundlich models with maximum adsorption capacity of  $142.80 \text{ mg}\cdot\text{g}^{-1}$ . The reusability tests clarified a good stability of CS@NZVI composite after three successive cycles.

#### 4. Removal of phosphate and nitrate

Recently, the proliferation of anions, especially phosphate and nitrate onto water bodies have become a serious problem (Lazaratou et al., 2020; Hashim et al., 2021). Although phosphate and nitrate are widely utilized as nutrients for all living beings (Mitra et al., 2020; Romero-Perdomo et al., 2021; Barbosa da Silva et al., 2020), discharge of these anions into water bodies definitely deteriorate the ecological system (Wang and Wei, 2021; Keshvaroostchokami et al., 2021). In addition, nitrate has a diverse impact on human health, at which the presence of nitrate in drinking water could cause blue baby syndrome in addition to the carcinogenic nitrosamide and nitrosamine. Thus, WHO authorized that the concentrations of phosphate and nitrate should not exceed  $5 \text{ mg}\cdot\text{L}^{-1}$  and  $50 \text{ mg}\cdot\text{L}^{-1}$ , respectively (Organization, 2004).

Removal of these hazard anions from water bodies is a sensible matter to preserve the environment. Among the adsorbent materials that have been developed to remove phosphate and nitrate ions are chitosan and its derivatives. Table 3 summarizes some attempts that have been executed to ameliorate the adsorption behavior of chitosan to be an auspicious adsorbent for removing phosphate and nitrate ions.

**Table 3** List of various adsorbents-based chitosan for removing of anions from their aqueous solutions.

Adsorbent	Adsorbate	$q_m (\text{mg}\cdot\text{g}^{-1})$	Ref.
La <sup>3+</sup> -bentonite/chitosan composite	Phosphate	23.52	(Xu et al., 2020)
Fe <sup>3+</sup> loaded chitosan/alginate hybrid beads	Phosphate	84.74	(Karthikeyan et al., 2019)
Chitosan/Al <sub>2</sub> O <sub>3</sub> /Fe <sub>3</sub> O <sub>4</sub> nanofibrous	Phosphate	135.10	(Bozorgpour et al., 2016)
Chitosan/Al <sub>2</sub> O <sub>3</sub> /Fe <sub>3</sub> O <sub>4</sub> beads	Phosphate	61.90	(Bozorgpour et al., 2016)
Zr(IV)- chitosan beads	Phosphate	60.60	(Liu and Zhang, 2015)
Quaternary amine modified chitosan beads	Phosphate	59.00	(Sowmya and Meenakshi, 2013)
KOH deacetylated calcite-chitosan based adsorbent	Phosphate	21.56	(Pap et al., 2020)
La-CS@PDA	Phosphate	195.30	(Zhao et al., 2020)
Chitosan encapsulated magnetic kaolin beads	Phosphate	92.05	(Karthikeyan and Meenakshi, 2021)
Cross-linked chitosan bead	Phosphate	52.10	(Mahaninia and Wilson, 2017)
Chitosan-magnetic kaolin beads	Nitrate	74.11	(Karthikeyan and Meenakshi, 2021)
La <sup>3+</sup> incorporated chitosan membrane	Nitrate	62.60	(Karthikeyan et al., 2019)
Chitosan quaternized resin	Nitrate	84.09	(Banu and Meenakshi, 2017)
PEG/chitosan	Nitrate	50.68	(Rajeswari et al., 2016)
PVA/chitosan	Nitrate	35.03	(Rajeswari et al., 2016)
Fe <sub>3</sub> O <sub>4</sub> /ZrO <sub>2</sub> /chitosan nanocomposite	Nitrate	89.30	(Jiang et al., 2013)
Cross-linked chitosan supported by biomass-derived carbon	Nitrate	12.40	(Salman Tabrizi and Yavari, 2020)
Chitosan hydrogel beads	Nitrate	92.10	(Chatterjee and Woo, 2009)

#### 4.1. Removal of phosphate anions

In this regard, Xu et al. (2020) applied a simple and scalable method for the fabrication of La-doped bentonite/chitosan composite (La-bent/CS). It was elucidated that the as-fabricated La-bent/CS composite provided a fast and high efficient behavior in the adsorptive removal of phosphate from an aqueous solution. Furthermore, La-bent/CS composite revealed a good anti-interference for the coexisting anions such as  $\text{NO}_3^-$ ,  $\text{Cl}^-$  and  $\text{SO}_4^{2-}$  at which these foreign species caused a slight decreased in the removal efficiency of phosphate. It was presented great ability of La-bent/CS composite to be recycled and reused for five sequential cycles with maintaining the removal efficiency of phosphate above 89%. Moreover, kinetics and isotherms study indicated that the adsorption data fitted pseudo-second order and Freundlich model, respectively. In addition, it was postulated that the adsorption mechanism of phosphate onto La-bent/CS composite occurred via electrostatic interaction, co-precipitation and complexation.

In yet another attempt, Karthikeyan et al. (2019) examined the removal of phosphate by using  $\text{Fe}^{3+}$  loaded chitosan-alginate biopolymeric hybrid beads (Fe-CS-SA). Intensive study was executed to determine the best conditions of the phosphate adsorption onto the fabricated beads. It was investigated that the apt pH to adsorb phosphate onto Fe-CS-SA beads was found to be between 3 and 6 where phosphate naturally represents in multi-forms;  $\text{H}_3\text{PO}_4$  ( $\text{pH} < 2$ ),  $\text{H}_2\text{PO}_4^-$  ( $\text{pH} 2-7$ ),  $\text{HPO}_4^{2-}$  ( $\text{pH} 7-11$ ) and  $\text{PO}_4^{3-}$  ( $\text{pH} > 11$ ) as clarified in Fig. 9. Subsequently, at low pH a strong columbic interaction occurs between the protonated COOH, OH and  $\text{NH}_2$  groups of Fe-CS-SA beads and the phosphate ions. However, the poor adsorption of phosphate ions at high pH could be due to the strong competition between the abundant  $\text{OH}^-$  ions and phosphate ions towards the surface of the beads.

Moreover, the impact of the interfering anions (viz.,  $\text{SO}_4^{2-}$ ,  $\text{Cl}^-$  and  $\text{HCO}_3^-$ ) on the adsorption of phosphate ions onto

Fe-CS-SA beads was inspected. The result clarified that the divalent  $\text{SO}_4^{2-}$  ions diminished the adsorption capacity of phosphate more than the univalent  $\text{Cl}^-$  and  $\text{HCO}_3^-$  owing to the higher charge density of  $\text{SO}_4^{2-}$  ions, rendering their adsorption onto Fe-CS-SA beads quicker than  $\text{Cl}^-$  and  $\text{HCO}_3^-$  ions. The kinetics study pointed out that the adsorption of phosphate ions onto Fe-CS-SA beads obeyed pseudo-second order and intra-particle diffusion models, while the isotherms study revealed that the studied adsorption process followed Freundlich model. The computed  $q_{\max}$  of phosphate ions onto Fe-CS-SA beads under Langmuir model was  $84.74 \text{ mg}\cdot\text{g}^{-1}$ . It is worthy to mention that the hypothetical mechanism of the adsorption of phosphate ions onto Fe-CS-SA occurred via the electrostatic interaction between phosphate ions and the protonated  $\text{COOH}$ ,  $\text{OH}$  and  $\text{NH}_2$  groups on the matrix of the beads at a high acidic medium. Also, the inner-sphere complexation may occur via the interaction of  $\text{Fe}(\text{OH})_3^+$  with phosphate ions as well as the ion exchange between  $\text{Cl}^-$  and phosphate greatly participated on the adsorption process.

In another study, Sowmya and Meenakshi (2013) focused on improving the efficiency and the renewability of chitosan. Quaternary amine-modified chitosan beads (QCS) were synthesized via the cross-linking of chitosan beads and glycidyl trimethyl ammonium chloride. The fabricated QCS beads revealed an enhanced adsorption behavior towards the adsorption of phosphate ions at which  $q_{\max}$  was found to be  $59 \text{ mg}\cdot\text{g}^{-1}$ . Besides, the fabricated beads exhibited ultrahigh renewability with the removal efficiency to be 97.5% after the 10th consequential adsorption/desorption cycles. Therefore, it was significant to study the mechanism of adsorption and desorption of phosphate. It was presumed that the adsorption/desorption mechanism of phosphate ions is essentially controlled by ions exchange mechanism. During the adsorption process  $\text{Cl}^-$  ions of QCS beads are replaced by phosphate ions. Whereas, the phosphate desorption from the beads occurred by exchanging the adsorbed phosphate ions by  $\text{Cl}^-$  ions of the eluent solution (NaCl) used to regenerate the beads.

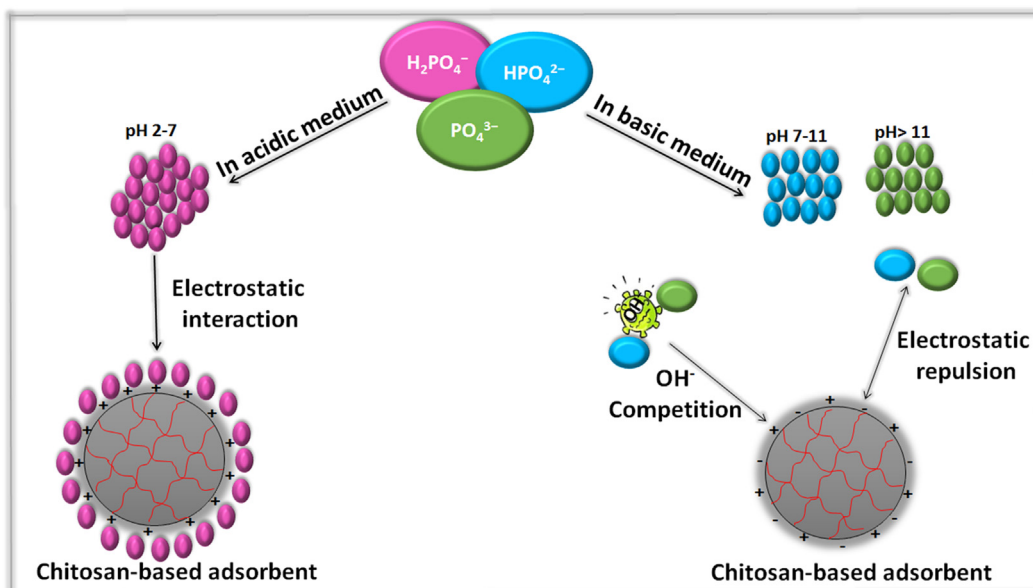


**Fig. 9** Schematic representation of the multi-forms of phosphate anion at different pH.

#### 4.2. Removal of nitrate

Karthikeyan and Meenakshi (2021), reported the fabrication of novel eco-friendly magnetic kaolin-chitosan beads (MK-CS) for removing nitrate ions from wastewater. The optimum conditions of the nitrate adsorption process onto MK-CS beads were investigated in a batch mode. Essentially, pH is the most predominant parameter in the adsorption process, so the adsorption of nitrate ions onto MK-CS beads was examined at different pH media. The results pointed out that the higher adsorption capacity of nitrate ions onto the beads at pH range 3–7 due to the strong attraction force between the anionic nitrate ions and the positively charged MK-CS beads. Thence, it was suggested that the adsorption of nitrate ions onto MK-CS beads controlled by the electrostatic interaction mechanism at which metal, metal oxide and amino groups spontaneously attracted nitrate ions from their aqueous solution. Besides, the presence of metal oxides in a hydrated form (i.e.  $Mg(OH)_2^+$ ,  $Fe(OH)_3^+$ ,  $Si(OH)_3^+$ ,  $Al(OH)_3^+$  and  $Na(OH)_2^+$ ) might form a network with nitrate via the surface complexation. Furthermore, it was expected that  $OH^-$  ions on the surface of the beads can be exchanged by nitrate ions via ligand exchange mechanism. In this context, Banu and coworker (Banu and Meenakshi, 2017), reported that the adsorption mechanism of nitrate ions onto the as-fabricated chitosan quaternized resin involves ion-exchange and electrostatic interaction. In addition, the possibility of the formation H-bond between nitrate ions and  $OH^-$  groups in the side chain of chitosan quaternized resin ( $NO_3^- \cdots OH^-$ ) was reported earlier by Mohan and coworkers (Mohan et al., 2010). Moreover, the competition effect of the coexisting anions such as  $SO_4^{2-}$ ,  $Cl^-$  and  $HCO_3^-$  on the nitrate adsorption process was explicitly investigated. It was found that the existence of  $SO_4^{2-}$  dramatically decreased the adsorption capacity of nitrate ions, indicating the great competition between  $SO_4^{2-}$  and nitrate ions. On the contrary, the tenuous competition between the monovalent

coexisting anions and nitrate was asserted from the insubstantial decrease in the nitrate adsorption capacity in the presence of  $HCO_3^-$  and  $Cl^-$ . These anticipated results can be ascribed to the faster charge density of multivalent anions renders them reach to the adsorbent surface prompter than monovalent anions.

In yet another attempt, Rajeswari et al. (2016), highlighted developing the adsorption capacity of chitosan with both polyethylene glycol and polyvinyl alcohol. It was inferred that the higher adsorption capacity of nitrate ions onto both composites was at pH 3, reflecting the strong electrostatic interaction between nitrate ions and the positively charged sites of PEG/CS and PVA/CS composites (Fig. 10a, b). However, the removal percentage of nitrate drastically decreased at a high basic medium which can be anticipated by the strong repulsion force between nitrate ions and the negatively charged sites of both composites. Besides, the maximum adsorption capacity of nitrate ions onto PEG/CS ( $50.68\text{ mg}\cdot\text{g}^{-1}$ ) was found to be higher than PVA/CS ( $30\text{ mg}\cdot\text{g}^{-1}$ ). The fabricated PEG/CS and PVA/CS composites showed amazing regeneration ability when an alkaline eluent is utilized to desorb nitrate from the surface of both composites.

#### 5. Summary

From our point of view, incorporating magnetic materials into the chitosan matrix and shaping chitosan in various forms like beads, membranes, hydrogel, etc., greatly boosts the separation problem of chitosan. Furthermore, the modification of chitosan with promising materials that possess high adsorbability such as metal–organic frameworks, layered double hydroxides, carbon materials, clays, etc. is an excellent solution to overcome the low adsorption capacity of chitosan. In addition, the functionalization of chitosan with suitable functional groups to attract the pollutants from their bulk

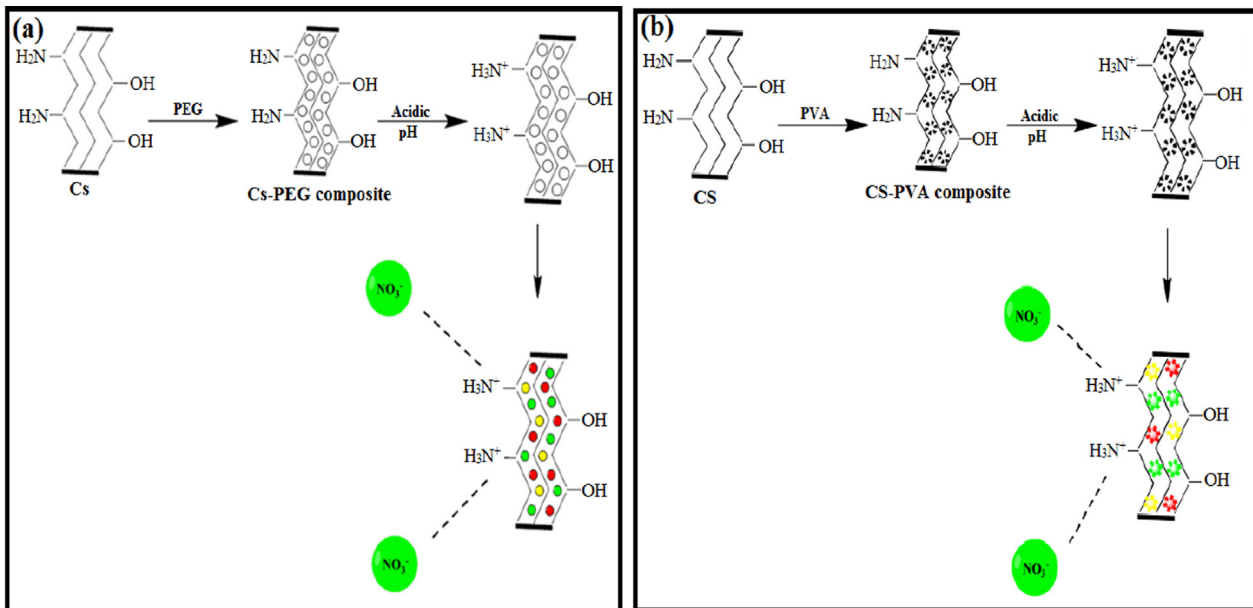


**Fig. 10** (a) Mechanism for the effect of pH on PEG/chitosan composite and (b) PVA/chitosan composite. Reprinted with permission from (Rajeswari et al., 2016); Copyright 2021, Elsevier.

**Table 4** Brief summary clarified the optimum pH, proposed adsorption mechanisms and the most common modifications.

Adsorbate	Opt. pH	Common modifications	Plausible adsorption mechanism
Arsenic	6–9	<ul style="list-style-type: none"> <li>• Multivalent metals-modified CS</li> <li>• Carbon materials-modified CS</li> <li>• Zeolite-modified CS</li> <li>• Magnetic CS</li> <li>• Clay-modified CS</li> </ul>	Electrostatic interactions, Ion exchange, Complexation, Reduction process
Copper	5–7	<ul style="list-style-type: none"> <li>• Zeolite-modified CS</li> <li>• Carbon materials-modified CS</li> <li>• Polymers-modified CS</li> <li>• Functionalized CS</li> <li>• Grafting CS</li> <li>• Clay-modified CS</li> </ul>	
Chromium	2–5	<ul style="list-style-type: none"> <li>• MOFs-modified CS</li> <li>• Multivalent metals-modified CS</li> <li>• Metal oxides-modified CS</li> <li>• Functionalized CS</li> <li>• Clay-modified CS</li> <li>• Magnetic CS</li> </ul>	
Lead	5–8.3	<ul style="list-style-type: none"> <li>• Polymers-modified CS</li> <li>• Magnetic CS</li> <li>• Grafting CS</li> <li>• Metal oxides-modified CS</li> </ul>	
Cadmium	5–8	<ul style="list-style-type: none"> <li>• Functionalized CS</li> <li>• Ion imprinted CS</li> <li>• Polymers-modified CS</li> <li>• Multivalent metals-modified CS</li> <li>• Metal oxides/ferrites-modified CS</li> </ul>	
Phosphate	3–7	<ul style="list-style-type: none"> <li>• Multivalent metals-modified CS</li> <li>• Polymers-modified CS</li> <li>• Functionalized CS</li> <li>• Clay-modified CS</li> <li>• Magnetic CS</li> <li>• Zeolite-modified CS</li> </ul>	Ion/Ligand exchange, Complexation, Electrostatic interaction, H-bonding
Nitrate	3–7	<ul style="list-style-type: none"> <li>• Clay-modified CS</li> <li>• Magnetic CS</li> <li>• Multivalent metals-modified CS</li> <li>• Functionalized CS</li> </ul>	

solutions via electrostatic interaction is the best technique to enhance chitosan selectivity.

The optimum pH, the proposed adsorption mechanisms and the recent modification techniques are summarized in Table 4.

## 6. Conclusions

Chitosan-based adsorbents demonstrate acceptable adsorption profiles towards the adsorption of various pollutants. Nonetheless, they suffer significant drawbacks such as the limited surface area, little adsorption capacity and lack of reusability. The presence of active amine and hydroxyl functional groups in chitosan biopolymer can assist in the combination of chitosan with other support materials, improving the physical and chemical properties of chitosan. This review highlighted the current advances of chitosan-based adsorbents and their adsorption aptitudes toward some toxic heavy metals, in specific; As(III), As(V), Cu(II), Cr(VI), Pb(II) and Cd(II) ions. Moreover, the capabilities of chitosan-based adsorbents for the adsorptive removal of phosphate and nitrate anions were also highlighted. The optimum adsorption conditions were discussed, clarifying the optimum pH to remove these contaminants, suitable adsorbent dose and system temperature. Furthermore, the adsorption mechanisms of these contami-

nants onto chitosan-based adsorbents were discussed. We can conclude that improving the adsorption capacity and enhancing the reuse property of chitosan-based adsorbents mainly depend on the type of modification as well as the adsorption conditions. The proposed mechanisms for the adsorption of these heavy metals as well as phosphate and nitrate anions involve several interactions such as electrostatic interactions, hydrogen bonding, ion exchanging and chemical binding.

### 6.1. Gap of knowledge and future perspectives

Indeed, researchers have faced various challenges regarding the adsorptive removal of heavy metals and anions by chitosan based-adsorbents. Some of these challenges and future recommendations are summarized as follows:

It is inevitable to infer the application viability of the developed chitosan-based adsorbents by boosting their adsorption performance and renewability, as well as diminishing their operation time.

The leaching probability of the developed chitosan-based adsorbents needs extensive investigation to avoid their leakage over the long term.

A plethora of pollutants exist in the real wastewater even with heavy metals or anions, so it is crucial to study the adsorption selectivity of the developed chitosan-based adsorbents.

Adequate study to the economy and the market is recommended; hence, the most important future goal is to execute the adsorption processes of heavy metals and anions at an industrial scale.

### Declaration of Competing Interest

The authors declare that they have no known competing financial interests or personal relationships that could have appeared to influence the work reported in this paper.

### References

- Abdelfatah, A.M., Fawzy, M., Eltaweil, A.S., El-Khouly, M.E., 2021. Green synthesis of nano-zero-valent iron using *ricinus communis* seeds extract: characterization and application in the treatment of methylene blue-polluted water. *ACS Omega*.
- Abdollahi, M., Zeinali, S., Nasirimoghaddam, S., Sabbaghi, S., 2015. Effective removal of As (III) from drinking water samples by chitosan-coated magnetic nanoparticles. *Desalin. Water Treat.* 56, 2092–2104.
- Adelolu, S.B., Khan, S., Patti, A.F., 2021. Arsenic contamination of groundwater and its implications for drinking water quality and human health in under-developed countries and remote communities—a review. *Appl. Sci.* 11, 1926.
- Ahmadi, M., Foladivanda, M., Jaafarzadeh, N., Ramezani, Z., Ramavandi, B., Jorfi, S., Kakavandi, B., 2017. Synthesis of chitosan zero-valent iron nanoparticles-supported for cadmium removal: characterization, optimization and modeling approach. *J. Water Supply: Res. Technol.—Aqua* 66, 116–130.
- Ahmed, M., Hameed, B., Hummadi, E., 2020. Review on recent progress in chitosan/chitin-carbonaceous material composites for the adsorption of water pollutants. *Carbohydr. Polym.* 116690.
- Al Sharabati, M., Abokwiek, R., Al-Othman, A., Tawalbeh, M., Karaman, C., Orooji, Y., Karimi, F., 2021. Biodegradable polymers and their nano-composites for the removal of endocrine-disrupting chemicals (EDCs) from wastewater: a review. *Environ. Res.* 111694.
- Ao, L., Xia, F., Ren, Y., Xu, J., Shi, D., Zhang, S., Gu, L., He, Q., 2019. Enhanced nitrate removal by micro-electrolysis using Fe0 and surfactant modified activated carbon. *Chem. Eng. J.* 357, 180–187.
- Asadi, S., Eris, S., Azizian, S., 2018. Alginate-based hydrogel beads as a biocompatible and efficient adsorbent for dye removal from aqueous solutions. *ACS Omega* 3, 15140–15148.
- Asgari, E., Sheikhmohammadi, A., Yeganeh, J., 2020. Application of the Fe3O4-chitosan nano-adsorbent for the adsorption of metronidazole from wastewater: optimization, kinetic, thermodynamic and equilibrium studies. *Int. J. Biol. Macromol.* 164, 694–706.
- Ayati, A., Tanhaei, B., Sillanpää, M., 2017. Lead (II)-ion removal by ethylenediaminetetraacetic acid ligand functionalized magnetic chitosan–aluminum oxide–iron oxide nanoadsorbents and microadsorbents: equilibrium, kinetics, and thermodynamics. *J. Appl. Polym. Sci.* 134.
- Ayub, A., Raza, Z.A., Majeed, M.I., Tariq, M.R., Irfan, A., 2020. Development of sustainable magnetic chitosan biosorbent beads for kinetic remediation of arsenic contaminated water. *Int. J. Biol. Macromol.* 163, 603–617.
- Babakhani, A., Sartaj, M., 2020. Removal of Cadmium (II) from aqueous solution using tripolyphosphate cross-linked chitosan. *J. Environ. Chem. Eng.* 8, 103842.
- Banu, H.T., Meenakshi, S., 2017. One pot synthesis of chitosan grafted quaternized resin for the removal of nitrate and phosphate from aqueous solution. *Int. J. Biol. Macromol.* 104, 1517–1527.
- Barbosa da Silva, G., de Mello Prado, R., Silva, S.L.O., Campos, C. N.S., Castellanos, L.G., Santos, L.C.N.D., Barreto, R.F., Teodoro, P.E., 2020. Nitrogen concentrations and proportions of ammonium and nitrate in the nutrition and growth of yellow passion fruit seedlings. *J. Plant Nutr.* 43, 2533–2547.
- Bhattacharyya, K.G., Gupta, S.S., 2008. Adsorption of a few heavy metals on natural and modified kaolinite and montmorillonite: a review. *Adv. Colloid Interface Sci.* 140, 114–131.
- Boddu, V.M., Abburi, K., Talbott, J.L., Smith, E.D., Haasch, R., 2008. Removal of arsenic (III) and arsenic (V) from aqueous medium using chitosan-coated biosorbent. *Water Res.* 42, 633–642.
- Bouyahmed, F., Cai, M., Reinert, L., Duclaux, L., Dey, R.K., Youcef, H.B., Lahcini, M., Muller, F., Delpeux-Ouldriane, S., 2018. A wide adsorption range hybrid material based on chitosan, activated carbon and montmorillonite for water treatment. *C—J. Carbon Res.* 4, 35.
- Bozorgpour, F., Ramandi, H.F., Jafari, P., Samadi, S., Yazd, S.S., Aliabadi, M., 2016. Removal of nitrate and phosphate using chitosan/Al2O3/Fe3O4 composite nanofibrous adsorbent: comparison with chitosan/Al2O3/Fe3O4 beads. *Int. J. Biol. Macromol.* 93, 557–565.
- Cai, W., Zhu, F., Liang, H., Jiang, Y., Tu, W., Cai, Z., Wu, J., Zhou, J., 2019. Preparation of thiourea-modified magnetic chitosan composite with efficient removal efficiency for Cr (VI). *Chem. Eng. Res. Des.* 144, 150–158.
- Cao, J., He, G., Ning, X., Wang, C., Fan, L., Yin, Y., Cai, W., 2021. Hydroxypropyl chitosan-based dual self-healing hydrogel for adsorption of chromium ions. *Int. J. Biol. Macromol.* 174, 89–100.
- Chatterjee, S., Woo, S.H., 2009. The removal of nitrate from aqueous solutions by chitosan hydrogel beads. *J. Hazard. Mater.* 164, 1012–1018.
- Chen, Y., Cai, W., Dang, C., Fan, J., Zhou, J., Liu, Z., 2020. A facile sol–gel synthesis of chitosan-boehmite film with excellent acid resistance and adsorption performance for Pb (II). *Chem. Eng. Res. Des.* 161, 332–339.
- Chen, D., Li, W., Wu, Y., Zhu, Q., Lu, Z., Du, G., 2013. Preparation and characterization of chitosan/montmorillonite magnetic microspheres and its application for the removal of Cr (VI). *Chem. Eng. J.* 221, 8–15.
- Chen, L., Wu, P., Chen, M., Lai, X., Ahmed, Z., Zhu, N., Dang, Z., Bi, Y., Liu, T., 2018. Preparation and characterization of the eco-friendly chitosan/vermiculite biocomposite with excellent removal capacity for cadmium and lead. *Appl. Clay Sci.* 159, 74–82.
- Chen, A., Zeng, G., Chen, G., Hu, X., Yan, M., Guan, S., Shang, C., Lu, L., Zou, Z., Xie, G., 2012. Novel thiourea-modified magnetic ion-imprinted chitosan/TiO2 composite for simultaneous removal of cadmium and 2, 4-dichlorophenol. *Chem. Eng. J.* 191, 85–94.
- Cho, D.-W., Jeon, B.-H., Chon, C.-M., Kim, Y., Schwartz, F.W., Lee, E.-S., Song, H., 2012. A novel chitosan/clay/magnetite composite for adsorption of Cu (II) and As (V). *Chem. Eng. J.* 200, 654–662.
- Choong, T.S., Chuah, T., Robiah, Y., Koay, F.G., Azni, I., 2007. Arsenic toxicity, health hazards and removal techniques from water: an overview. *Desalination* 217, 139–166.
- N.R. Council, Arsenic in Drinking Water, 1999.
- Crini, G., 2005. Recent developments in polysaccharide-based materials used as adsorbents in wastewater treatment. *Prog. Polym. Sci.* 30, 38–70.
- Crini, G., 2006. Non-conventional low-cost adsorbents for dye removal: a review. *Bioresour. Technol.* 97, 1061–1085.
- Crini, G., Badot, P.-M., 2011. Sorption Processes and Pollution: Conventional and Non-conventional Sorbents for Pollutant Removal from Wastemasters. Presses Univ. Franche-Comté.
- Cui, H., Chen, J., Yang, H., Wang, W., Liu, Y., Zou, D., Liu, W., Men, G., 2013. Preparation and application of Aliquat 336 functionalized chitosan adsorbent for the removal of Pb (II). *Chem. Eng. J.* 232, 372–379.
- Cunha, B.S., Bataglioli, R.A., Taketa, T.B., Lopes, L.M., Beppu, M. M., 2019. Ionic liquid functionalization of chitosan beads for improving thermal stability and copper ions uptake from aqueous solution. *J. Environ. Chem. Eng.* 7, 103181.

- Dai, Y., Sun, Q., Wang, W., Lu, L., Liu, M., Li, J., Yang, S., Sun, Y., Zhang, K., Xu, J., 2018. Utilizations of agricultural waste as adsorbent for the removal of contaminants: a review. *Chemosphere* 211, 235–253.
- de Souza, T.N.V., de Carvalho, S.M.L., Vieira, M.G.A., da Silva, M. G.C., Brasil, D.d.S.B., 2018. Adsorption of basic dyes onto activated carbon: experimental and theoretical investigation of chemical reactivity of basic dyes using DFT-based descriptors. *Appl. Surf. Sci.* 448, 662–670.
- Dehghani, M.H., Sanaei, D., Ali, I., Bhatnagar, A., 2016. Removal of chromium (VI) from aqueous solution using treated waste newspaper as a low-cost adsorbent: kinetic modeling and isotherm studies. *J. Mol. Liq.* 215, 671–679.
- Dinh, V.-P., Le, N.-C., Tuyen, L.A., Hung, N.Q., Nguyen, V.-D., Nguyen, N.-T., 2018. Insight into adsorption mechanism of lead (II) from aqueous solution by chitosan loaded MnO<sub>2</sub> nanoparticles. *Mater. Chem. Phys.* 207, 294–302.
- Dinh, V.-P., Nguyen, M.-D., Nguyen, Q.H., Luu, T.-T., Luu, A.T., Tap, T.D., Ho, T.-H., Phan, T.P., Nguyen, T.D., Tan, L., 2020. Chitosan-MnO<sub>2</sub> nanocomposite for effective removal of Cr (VI) from aqueous solution. *Chemosphere* 257, 127147.
- Dong, Q., Guo, X., Huang, X., Liu, L., Tallon, R., Taylor, B., Chen, J., 2019. Selective removal of lead ions through capacitive deionization: role of ion-exchange membrane. *Chem. Eng. J.* 361, 1535–1542.
- Dongre, R.S., Sadasivuni, K.K., Deshmukh, K., Mehta, A., Basu, S., Meshram, J.S., Al-Maadeed, M.A.A., Karim, A., 2019. Natural polymer based composite membranes for water purification: a review. *Polymer-Plastics Technol. Mater.* 58, 1295–1310.
- Dou, J., Gan, D., Huang, Q., Liu, M., Chen, J., Deng, F., Zhu, X., Wen, Y., Zhang, X., Wei, Y., 2019. Functionalization of carbon nanotubes with chitosan based on MALI multicomponent reaction for Cu<sup>2+</sup> removal. *Int. J. Biol. Macromol.* 136, 476–485.
- Duman, O., Polat, T.G., Diker, C.Ö., Tunç, S., 2020. Agar/κ-carrageenan composite hydrogel adsorbent for the removal of methylene blue from water. *Int. J. Biol. Macromol.* 160, 823–835.
- Eldin, M.M., Omer, A., Wassel, M., Tamer, T., Abd-Elmonem, M., Ibrahim, S., 2015. Novel smart pH sensitive chitosan grafted alginate hydrogel microcapsules for oral protein delivery: II. Evaluation of the swelling behavior. *Int. J. Pharmacy Pharmacol. Sci.* 7, 331–337.
- El-Monaem, E.M.A., El-Latif, M.M.A., Eltaweil, A.S., El-Subrui, G.M., 2021. Cobalt nanoparticles supported on reduced amine-functionalized graphene oxide for catalytic reduction of nitroanilines and organic dyes. *NANO* 2150039.
- El-sayed, H.A.-A., Motawea, E.A.-T., 2020. Optimization and adsorption behavior of nanostructured NiFe<sub>2</sub>O<sub>4</sub>/Poly AMPS grafted biopolymer. *J. Polym. Environ.* 28, 2335–2351.
- El-Sayed, E., Tamer, T., Omer, A., Mohy Eldin, M., 2016. Development of novel chitosan schiff base derivatives for cationic dye removal: methyl orange model. *Desalin. Water Treat.* 57, 22632–22645.
- El-Subrui, G., Eltaweil, A., Sallam, S., 2019. Synthesis of active MFe<sub>2</sub>O<sub>4</sub>/γ-Fe<sub>2</sub>O<sub>3</sub> nanocomposites (metal= Ni or Co) for reduction of nitro-containing pollutants and methyl orange degradation. *NANO* 14, 1950125.
- Eltaweil, A.S., Abd El-Monaem, E.M., Omer, A.M., Khalifa, R.E., Abd El-Latif, M.M., El-Subrui, G.M., 2020. Efficient removal of toxic methylene blue (MB) dye from aqueous solution using a metal-organic framework (MOF) MIL-101 (Fe): isotherms, kinetics, and thermodynamic studies. *Desalin. Water Treat.* 189, 395–407.
- Eltaweil, A.S., Abd El-Monaem, E.M., El-Subrui, G.M., Abd El-Latif, M.M., Omer, A.M., 2020. Fabrication of UiO-66/MIL-101 (Fe) binary MOF/carboxylated-GO composite for adsorptive removal of methylene blue dye from aqueous solutions, *RSC Advances* 10, 19008–19019.
- Eltaweil, A.S., Elgarhy, G.S., El-Subrui, G.M., Omer, A.M., 2020. Carboxymethyl cellulose/carboxylated graphene oxide composite microbeads for efficient adsorption of cationic methylene blue dye. *Int. J. Biol. Macromol.* 154, 307–318.
- Eltaweil, A.S., El-Monaem, E.M.A., Mohy-Eldin, M.S., Omer, A.M., 2021. Fabrication of attapulgite/magnetic aminated chitosan composite as efficient and reusable adsorbent for Cr (VI) ions. *Sci. Rep.* 11, 1–15.
- Eltaweil, A.S., Mamdouh, I.M., Abd El-Monaem, E.M., El-Subrui, G.M., 2021. Highly efficient removal for methylene blue and Cu<sup>2+</sup> onto UiO-66 metal-organic framework/carboxylated graphene oxide-incorporated sodium alginate beads. *ACS Omega*.
- Eltaweil, A.S., Mamdouh, I.M., Abd El-Monaem, E.M., El-Subrui, G.M., 2021. Highly efficient removal for methylene blue and Cu<sup>2+</sup> onto UiO-66 metal-organic framework/carboxylated graphene oxide-incorporated sodium alginate beads. *ACS Omega* 6, 23528–23541.
- Eltaweil, A., Mohamed, H.A., Abd El-Monaem, E.M., El-Subrui, G., 2020. Mesoporous magnetic biochar composite for enhanced adsorption of malachite green dye: characterization, adsorption kinetics, thermodynamics and isotherms. *Adv. Powder Technol.* 31, 1253–1263.
- Eltaweil, A.S., El-Tawil, A.M., Abd El-Monaem, E.M., El-Subrui, G.M., 2021. Zero valent iron nanoparticle-loaded nanobentonite intercalated carboxymethyl chitosan for efficient removal of both anionic and cationic dyes. *ACS Omega*.
- Eltaweil, A.S., Elshishini, H.M., Ghatass, Z.F., Elsubrui, G.M., 2021. Ultra-high adsorption capacity and selective removal of Congo red over aminated graphene oxide modified Mn-doped UiO-66 MOF. *Powder Technol.* 379, 407–416.
- Eltaweil, A.S., Omer, A.M., El-Aqapa, H.G., Gaber, N.M., Attia, N. F., El-Subrui, G.M., Mohy-Eldin, M.S., Abd El-Monaem, E.M., 2021. Chitosan based adsorbents for the removal of phosphate and nitrate: a critical review. *Carbohydr. Polym.*
- Eltaweil, A.S., El-Tawil, A.M., Abd El-Monaem, E.M., El-Subrui, G.M., 2021. Zero valent iron nanoparticle-loaded nanobentonite intercalated carboxymethyl chitosan for efficient removal of both anionic and cationic dyes. *ACS Omega* 6, 6348–6360.
- Fan, C., Li, K., Li, J., Ying, D., Wang, Y., Jia, J., 2017. Comparative and competitive adsorption of Pb (II) and Cu (II) using tetraethylenepentamine modified chitosan/CoFe<sub>2</sub>O<sub>4</sub> particles. *J. Hazard. Mater.* 326, 211–220.
- Gandhi, M.R., Meenakshi, S., 2012. Preparation and characterization of silica gel/chitosan composite for the removal of Cu (II) and Pb (II). *Int. J. Biol. Macromol.* 50, 650–657.
- Gao, C., Wang, X.-L., An, Q.-D., Xiao, Z.-Y., Zhai, S.-R., 2021. Synergistic preparation of modified alginate aerogel with melamine/chitosan for efficiently selective adsorption of lead ions. *Carbohydr. Polym.* 256, 117564.
- Geisse, A.R., Ngule, C.M., Genna, D.T., 2020. Removal of lead ions from water using thiophene-functionalized metal-organic frameworks. *Chem. Commun.* 56, 237–240.
- Godt, J., Scheidig, F., Grosse-Siestrup, C., Esche, V., Brandenburg, P., Reich, A., Groneberg, D.A., 2006. The toxicity of cadmium and resulting hazards for human health. *J. Occupat. Med. Toxicol.* 1, 1–6.
- Goel, P., 2006. Water Pollution: Causes, Effects and Control. New Age International.
- Gogoi, P., Thakur, A.J., Devi, R.R., Das, B., Maji, T.K., 2017. Adsorption of As (V) from contaminated water over chitosan coated magnetite nanoparticle: equilibrium and kinetics study. *Environ. Nanotechnol. Monit. Manage.* 8, 297–305.
- Gokila, S., Gomathi, T., Sudha, P., Anil, S., 2017. Removal of the heavy metal ion chromium (VI) using Chitosan and Alginate nanocomposites. *Int. J. Biol. Macromol.* 104, 1459–1468.
- Gomez-Maldonado, D., Erramuspe, I.B.V., Peresin, M.S., 2019. Natural polymers as alternative adsorbents and treatment agents for water remediation. *BioResources* 14, 10093–10160.

- Guo, D.-M., An, Q.-D., Xiao, Z.-Y., Zhai, S.-R., Yang, D.-J., 2018. Efficient removal of Pb (II), Cr (VI) and organic dyes by polydopamine modified chitosan aerogels. *Carbohydr. Polym.* 202, 306–314.
- Guo, C., Wang, Y., Wang, F., Wang, Y., 2021. Adsorption performance of amino functionalized magnetic molecular sieve adsorbent for effective removal of lead ion from aqueous solution. *Nanomaterials* 11, 2353.
- Gupta, A., Chauhan, V.S., Sankararamakrishnan, N., 2009. Preparation and evaluation of iron–chitosan composites for removal of As (III) and As (V) from arsenic contaminated real life groundwater. *Water Res.* 43, 3862–3870.
- Gupta, A., Yunus, M., Sankararamakrishnan, N., 2012. Zerovalent iron encapsulated chitosan nanospheres—A novel adsorbent for the removal of total inorganic Arsenic from aqueous systems. *Chemosphere* 86, 150–155.
- Han, C., Yang, T., Liu, H., Yang, L., Luo, Y., 2019. Characterizations and mechanisms for synthesis of chitosan-coated Na-X zeolite from fly ash and As (V) adsorption study. *Environ. Sci. Pollut. Res.* 26, 10106–10116.
- Hashim, K.S., Ewadh, H.M., Muhsin, A.A., Zubaidi, S.L., Kot, P., Muradov, M., Aljefery, M., Al-Khaddar, R., 2021. Phosphate removal from water using bottom ash: adsorption performance, coexisting anions and modelling studies. *Water Sci. Technol.* 83, 77–89.
- He, Y., Gou, S., Zhou, L., Tang, L., Liu, T., Liu, L., Duan, M., 2021. Amidoxime-functionalized polyacrylamide-modified chitosan containing imidazoline groups for effective removal of Cu<sup>2+</sup> and Ni<sup>2+</sup>. *Carbohydr. Polym.* 252, 117160.
- He, W., Yu, Q., Wang, N., Ouyang, X.-K., 2020. Efficient adsorption of Cu (II) from aqueous solutions by acid-resistant and recyclable ethylenediamine tetraacetic acid-grafted polyvinyl alcohol/chitosan beads. *J. Mol. Liq.* 316, 113856.
- Hosseinzadeh, H., Ramin, S., 2018. Effective removal of copper from aqueous solutions by modified magnetic chitosan/graphene oxide nanocomposites. *Int. J. Biol. Macromol.* 113, 859–868.
- Hu, D., Lian, Z., Xian, H., Jiang, R., Wang, N., Weng, Y., Peng, X., Wang, S., Ouyang, X.K., 2020. Adsorption of Pb (II) from aqueous solution by polyacrylic acid grafted magnetic chitosan nanocomposite. *Int. J. Biol. Macromol.* 154, 1537–1547.
- Hu, A., Yang, X., You, Q., Liu, Y., Wang, Q., Liao, G., Wang, D., 2019. Magnetically hyper-cross-linked polymers with well-developed mesoporous: a broad-spectrum and highly efficient adsorbent for water purification. *JMatS* 54, 2712–2728.
- Huang, Y., He, C., Shen, C., Guo, J., Mubeen, S., Yuan, J., Yang, Z., 2017. Toxicity of cadmium and its health risks from leafy vegetable consumption. *Food Funct.* 8, 1373–1401.
- Ibrahim, A.G., Saleh, A.S., Elsharma, E.M., Metwally, E., Siyam, T., 2019. Chitosan-g-maleic acid for effective removal of copper and nickel ions from their solutions. *Int. J. Biol. Macromol.* 121, 1287–1294.
- Inyinbor Adejumoke, A., Adebesin Babatunde, O., Oluyori Abimbola, P., Adelani Akande Tabitha, A., Dada Adewumi, O., Oreofe Toyin, A., 2018. Water pollution: effects, prevention, and climatic impact. *Water Challenges Urbanizing World* 33.
- Islam, M.M., Masum, S.M., Rahman, M.M., Molla, M.A.I., Shaikh, A., Roy, S., 2011. Preparation of chitosan from shrimp shell and investigation of its properties. *Int. J. Basic Appl. Sci.* 11, 77–80.
- Jain, M., Khan, S.A., Pandey, A., Pant, K.K., Ziora, Z.M., Blaskovich, M.A., 2021. Instructive analysis of engineered carbon materials for potential application in water and wastewater treatment. *Sci. Total Environ.* 148583.
- Jiang, Y., Cai, W., Tu, W., Zhu, M., 2018. Facile cross-link method to synthesize magnetic Fe3O4@SiO2–Chitosan with high adsorption capacity toward hexavalent chromium. *J. Chem. Eng. Data* 64, 226–233.
- Jiang, H., Chen, P., Luo, S., Tu, X., Cao, Q., Shu, M., 2013. Synthesis of novel nanocomposite Fe3O4/ZrO2/chitosan and its application for removal of nitrate and phosphate. *Appl. Surf. Sci.* 284, 942–949.
- Kalaimurugan, D., Durairaj, K., Kumar, A.J., Senthilkumar, P., Venkatesan, S., 2020. Novel preparation of fungal conidiophores biomass as adsorbent for removal of phosphorus from aqueous solution. *Environ. Sci. Pollut. Res.* 27, 20757–20769.
- Karim, M.R., Ajiaz, M.O., Alharth, N.H., Alharbi, H.F., Al-Mubaddel, F.S., Awual, M.R., 2019. Composite nanofibers membranes of poly (vinyl alcohol)/chitosan for selective lead (II) and cadmium (II) ions removal from wastewater. *Ecotoxicol. Environ. Saf.* 169, 479–486.
- Karimi, F., Ayati, A., Tanhaei, B., Sanati, A.L., Afshar, S., Kardan, A., Dabirifar, Z., Karaman, C., 2022. Removal of metal ions using a new magnetic chitosan nano-bio-adsorbent. A powerful approach in water treatment. *Environ. Res.* 203, 111753.
- Karimi-Maleh, H., Ranjbari, S., Tanhaei, B., Ayati, A., Orooji, Y., Alizadeh, M., Karimi, F., Salmanpour, S., Rouhi, J., Sillanpää, M., 2021. Novel 1-butyl-3-methylimidazolium bromide impregnated chitosan hydrogel beads nanostructure as an efficient nanobio-adsorbent for cationic dye removal: Kinetic study. *Environ. Res.* 195, 110809.
- Karthikeyan, P., Banu, H.A.T., Meenakshi, S., 2019. Synthesis and characterization of metal loaded chitosan-alginate biopolymeric hybrid beads for the efficient removal of phosphate and nitrate ions from aqueous solution. *Int. J. Biol. Macromol.* 130, 407–418.
- Karthikeyan, P., Banu, H.A.T., Meenakshi, S., 2019. Removal of phosphate and nitrate ions from aqueous solution using La<sup>3+</sup> incorporated chitosan biopolymeric matrix membrane. *Int. J. Biol. Macromol.* 124, 492–504.
- Karthikeyan, P., Meenakshi, S., 2021. Fabrication of hybrid chitosan encapsulated magnetic-kaolin beads for adsorption of phosphate and nitrate ions from aqueous solutions. *Int. J. Biol. Macromol.* 168, 750–759.
- Kaushal, A., Singh, S., 2017. Removal of heavy metals by nano-adsorbents: as review. *J. Environ. Biotechnol. Res.* 6, 96–104.
- Kentish, S.E., Stevens, G.W., 2001. Innovations in separations technology for the recycling and re-use of liquid waste streams. *Chem. Eng. J.* 84, 149–159.
- Keshvarroostchokami, M., Majidi, M., Zamani, A., Liu, B., 2021. A review on the use of chitosan and chitosan derivatives as the bio-adsorbents for the water treatment: Removal of nitrogen-containing pollutants. *Carbohydr. Polym.* 118625.
- Khalifa, R.E., Omer, A.M., Tamer, T.M., Salem, W.M., Eldin, M.M., 2019. Removal of methylene blue dye from synthetic aqueous solutions using novel phosphonate cellulose acetate membranes: adsorption kinetic, equilibrium, and thermodynamic studies. *Desalin. Water Treat.* 144, 272–285.
- Kloster, G.A., Valiente, M., Marcovich, N.E., Mosiewicki, M.A., 2020. Adsorption of arsenic onto films based on chitosan and chitosan/nano-iron oxide. *Int. J. Biol. Macromol.* 165, 1286–1295.
- Kobayashi, Y., Ogata, F., Nakamura, T., Kawasaki, N., 2020. Synthesis of novel zeolites produced from fly ash by hydrothermal treatment in alkaline solution and its evaluation as an adsorbent for heavy metal removal. *J. Environ. Chem. Eng.* 8, 103687.
- Kumar, A.S.K., Jiang, S.-J., 2016. Chitosan-functionalized graphene oxide: a novel adsorbent an efficient adsorption of arsenic from aqueous solution. *J. Environ. Chem. Eng.* 4, 1698–1713.
- Kumari, U., Siddiqi, H., Bal, M., Meikap, B., 2020. Calcium and zirconium modified acid activated alumina for adsorptive removal of fluoride: performance evaluation, kinetics, isotherm, characterization and industrial wastewater treatment. *Adv. Powder Technol.* 31, 2045–2060.
- Kyzas, G.Z., Bikaris, D.N., 2015. Recent modifications of chitosan for adsorption applications: a critical and systematic review. *Mar. Drugs* 13, 312–337.
- Kyzas, G.Z., Kostoglou, M., Lazaridis, N.K., Lambropoulou, D.A., Bikaris, D.N., 2013. Environmental friendly technology for the

- removal of pharmaceutical contaminants from wastewaters using modified chitosan adsorbents. *Chem. Eng. J.* 222, 248–258.
- Lazaratou, C., Vayenas, D., Papoulis, D., 2020. The role of clays, clay minerals and clay-based materials for nitrate removal from water systems: a review. *Appl. Clay Sci.* 185, 105377.
- Li, Q.-H., Dong, M., Li, R., Cui, Y.-Q., Xie, G.-X., Wang, X.-X., Long, Y.-Z., 2021. Enhancement of Cr (VI) removal efficiency via adsorption/photocatalysis synergy using electrospun chitosan/g-C<sub>3</sub>N<sub>4</sub>/TiO<sub>2</sub> nanofibers. *Carbohydr. Polym.* 253, 117200.
- Li, F., Fei, P., Cheng, B., Meng, J., Liao, L., 2019. Synthesis, characterization and excellent antibacterial property of cellulose acetate reverse osmosis membrane via a two-step reaction. *Carbohydr. Polym.* 216, 312–321.
- Li, T.-T., Liu, Y.-G., Peng, Q.-Q., Hu, X.-J., Liao, T., Wang, H., Lu, M., 2013. Removal of lead (II) from aqueous solution with ethylenediamine-modified yeast biomass coated with magnetic chitosan microparticles: Kinetic and equilibrium modeling. *Chem. Eng. J.* 214, 189–197.
- Li, N., Tian, Y., Zhao, J., Zhang, J., Zuo, W., Ding, Y., 2017. Efficient removal of chromium from water by Mn<sub>3</sub>O<sub>4</sub>@ZnO/Mn<sub>3</sub>O<sub>4</sub> composite under simulated sunlight irradiation: synergy of photocatalytic reduction and adsorption. *Appl. Catal. B* 214, 126–136.
- Li, S., Wang, D., Xiao, H., Zhang, H., Cao, S., Chen, L., Ni, Y., Huang, L., 2021. Ultra-low pressure cellulose-based nanofiltration membrane fabricated on layer-by-layer assembly for efficient sodium chloride removal. *Carbohydr. Polym.* 255, 117352.
- Liakos, E.V., Lazaridou, M., Michailidou, G., Koumentakou, I., Lambropoulou, D.A., Bikaris, D.N., Kyzas, G.Z., 2021. Chitosan adsorbent derivatives for pharmaceuticals removal from effluents: a review. *Macromol* 1, 130–154.
- Liang, X.X., Ouyang, X.-K., Wang, S., Yang, L.-Y., Huang, F., Ji, C., Chen, X., 2019. Efficient adsorption of Pb (II) from aqueous solutions using aminopropyltriethoxysilane-modified magnetic attapulgite@ chitosan (APTS-Fe3O4/APT@ CS) composite hydrogel beads. *Int. J. Biol. Macromol.* 137, 741–750.
- Liang, X.-X., Wang, N., Qu, Y.-L., Yang, L.-Y., Wang, Y.-G., Ouyang, X.-K., 2018. Facile preparation of metal-organic framework (MIL-125)/chitosan beads for adsorption of Pb (II) from aqueous solutions. *Molecules* 23, 1524.
- Liu, B., Kim, K.-H., Kumar, V., Kim, S., 2020. A review of functional sorbents for adsorptive removal of arsenic ions in aqueous systems. *J. Hazard. Mater.* 388, 121815.
- Liu, Y., Liu, Y., Huo, T., Wu, X., Wei, J., Pei, D., Di, D., Wang, J., Sun, Y., 2015. Effect of the ionic liquid group in novel interpenetrating polymer networks on the adsorption properties for oleuropein from aqueous solutions. *New J. Chem.* 39, 9181–9190.
- Liu, X., Zhang, L., 2015. Removal of phosphate anions using the modified chitosan beads: adsorption kinetic, isotherm and mechanism studies. *Powder Technol.* 277, 112–119.
- Lobo, C., Castellari, J., Lerner, J.C., Bertola, N., Zaritzky, N., 2020. Functional iron chitosan microspheres synthesized by ionotropic gelation for the removal of arsenic (V) from water. *Int. J. Biol. Macromol.* 164, 1575–1583.
- Lu, C., Yu, S., Yao, T., Zeng, C., Wang, C., Zhang, L., 2015. Zeolite X/chitosan hybrid microspheres and their adsorption properties for Cu (II) ions in aqueous solutions. *J. Porous Mater.* 22, 1255–1263.
- Ma, L., Shi, X., Zhang, X., Dong, S., Li, L., 2019. Electrospun cellulose acetate-polycaprolactone/chitosan core-shell nanofibers for the removal of Cr (VI). *Physica Status Solidi (a)* 216, 1900379.
- Mahaninia, M.H., Wilson, L.D., 2017. Phosphate uptake studies of cross-linked chitosan bead materials. *J. Colloid Interface Sci.* 485, 201–212.
- Mandal, B.K., Suzuki, K.T., 2002. Arsenic round the world: a review. *Talanta* 58, 201–235.
- Mitra, D., Anđelković, S., Panneerselvam, P., Senapati, A., Vasić, T., Ganeshamurthy, A., Chauhan, M., Uniyal, N., Mahakur, B., Radha, T., 2020. Phosphate-solubilizing microbes and biocontrol agent for plant nutrition and protection: current perspective. *Commun. Soil Sci. Plant Anal.* 51, 645–657.
- Mohan, N., Vijayalakshmi, K.P., Koga, N., Suresh, C.H., 2010. Comparison of aromatic NH···π, OH···π, and CH···π interactions of alanine using MP2, CCSD, and DFT methods. *J. Comput. Chem.* 31, 2874–2882.
- Mu, R., Liu, B., Chen, X., Wang, N., Yang, J., 2020. Adsorption of Cu (II) and Co (II) from aqueous solution using lignosulfonate/chitosan adsorbent. *Int. J. Biol. Macromol.* 163, 120–127.
- Mukhopadhyay, M., Lakhotia, S.R., Ghosh, A., Bindal, R., 2019. Removal of arsenic from aqueous media using zeolite/chitosan nanocomposite membrane. *Sep. Sci. Technol.* 54, 282–288.
- Muzzarelli, R.A.A., Tanfani, F., 1985. The N-permethylation of chitosan and the preparation of N-trimethyl chitosan iodide. *Carbohydr. Polym.* 5, 297–307.
- Nakakubo, K., Hasegawa, H., Ito, M., Yamazaki, K., Miyaguchi, M., Biswas, F.B., Ikai, T., Maeda, K., 2019. Dithiocarbamate-modified cellulose resins: a novel adsorbent for selective removal of arsenite from aqueous media. *J. Hazard. Mater.* 380, 120816.
- Naz, A., Arun, S., Narvi, S.S., Alam, M.S., Singh, A., Bhartiya, P., Dutta, P., 2018. Cu (II)-carboxymethyl chitosan-silane schiff base complex grafted on nano silica: structural evolution, antibacterial performance and dye degradation ability. *Int. J. Biol. Macromol.* 110, 215–226.
- Ngah, W.W., Teong, L., Hanafiah, M.M., 2011. Adsorption of dyes and heavy metal ions by chitosan composites: a review. *Carbohydr. Polym.* 83, 1446–1456.
- Ngwabebhoh, F.A., Erdem, A., Yildiz, U., 2016. Synergistic removal of Cu (II) and nitrazine yellow dye using an eco-friendly chitosan-montmorillonite hydrogel: optimization by response surface methodology. *J. Appl. Polym. Sci.* 133.
- Niu, C., Zhang, N., Hu, C., Zhang, C., Zhang, H., Xing, Y., 2021. Preparation of a novel citric acid-crosslinked Zn-MOF/chitosan composite and application in adsorption of chromium (VI) and methyl orange from aqueous solution. *Carbohydr. Polym.* 258, 117644.
- Omer, A.M., Elgarhy, G.S., El-Subrouti, G.M., Khalifa, R.E., Eltaweil, A.S., 2020. Fabrication of novel iminodiacetic acid-functionalized carboxymethyl cellulose microbeads for efficient removal of cationic crystal violet dye from aqueous solutions. *Int. J. Biol. Macromol.* 148, 1072–1083.
- Omer, A.M., Abd El-Monaem, E.M., Abd El-Latif, M.M., El-Subrouti, G.M., Eltaweil, A.S., 2021. Facile fabrication of novel magnetic ZIF-67 MOF@ aminated chitosan composite beads for the adsorptive removal of Cr (VI) from aqueous solutions. *Carbohydr. Polym.*, 118084.
- Omer, A.M., Ahmed, M.S., El-Subrouti, G.M., Khalifa, R.E., Eltaweil, A.S., 2021. pH-sensitive alginate/carboxymethyl chitosan/aminated chitosan microcapsules for efficient encapsulation and delivery of diclofenac sodium. *Pharmaceutics* 13, 338.
- Omer, A., Khalifa, R., Hu, Z., Zhang, H., Liu, C., Ouyang, X.-K., 2019. Fabrication of tetraethylenepentamine functionalized alginate beads for adsorptive removal of Cr (VI) from aqueous solutions. *Int. J. Biol. Macromol.* 125, 1221–1231.
- Omer, A., Khalifa, R., Tamer, T., Elnouby, M., Hamed, A., Ammar, Y., Ali, A., Gouda, M., Eldin, M.M., 2019. Fabrication of a novel low-cost superoleophilic nonanol chitosan-poly (butyl acrylate) grafted copolymer for the adsorptive removal of crude oil spills. *Int. J. Biol. Macromol.* 140, 588–599.
- W.H. Organization, 2004. The International Statistical Classification of Diseases and Health Related Problems ICD-10: Tenth Revision, vol. 1. Tabular List, World Health Organization.
- Pal, P., Pal, A., 2019. Treatment of real wastewater: Kinetic and thermodynamic aspects of cadmium adsorption onto surfactant-modified chitosan beads. *Int. J. Biol. Macromol.* 131, 1092–1100.
- Pap, S., Kirk, C., Bremner, B., Sekulic, M.T., Shearer, L., Gibb, S. W., Taggart, M.A., 2020. Low-cost chitosan-calcite adsorbent

- development for potential phosphate removal and recovery from wastewater effluent. *Water Res.* 173, 115573.
- Park, S., Gomez-Flores, A., Chung, Y.S., Kim, H., 2015. Removal of cadmium and lead from aqueous solution by hydroxyapatite/chitosan hybrid fibrous sorbent: kinetics and equilibrium studies. *J. Chem.* 2015.
- Peng, S., Meng, H., Ouyang, Y., Chang, J., 2014. Nanoporous magnetic cellulose–chitosan composite microspheres: preparation, characterization, and application for Cu (II) adsorption. *Ind. Eng. Chem. Res.* 53, 2106–2113.
- Pincus, L.N., Petrović, P.V., Gonzalez, I.S., Stavitski, E., Fishman, Z. S., Rudel, H.E., Anastas, P.T., Zimmerman, J.B., 2021. Selective adsorption of arsenic over phosphate by transition metal cross-linked chitosan. *Chem. Eng. J.* 412, 128582.
- Podgorski, J., Berg, M., 2020. Global threat of arsenic in groundwater. *Science* 368, 845–850.
- Pontoni, L., Fabbri, M., 2012. Use of chitosan and chitosan-derivatives to remove arsenic from aqueous solutions—a mini review. *Carbohydr. Res.* 356, 86–92.
- Prakash, N., Soundarajan, M., Vendan, S.A., Sudha, P., Renganathan, N., 2017. Contemplating the feasibility of vermiculate blended chitosan for heavy metal removal from simulated industrial wastewater. *Appl. Water Sci.* 7, 4207–4218.
- Pyrzynska, K., 2019. Removal of cadmium from wastewaters with low-cost adsorbents. *J. Environ. Chem. Eng.* 7, 102795.
- Qi, X., Wei, W., Su, T., Zhang, J., Dong, W., 2018. Fabrication of a new polysaccharide-based adsorbent for water purification. *Carbohydr. Polym.* 195, 368–377.
- Quiroga-Flores, R., Noshad, A., Wallenberg, R., Önnby, L., 2019. Adsorption of cadmium by a high-capacity adsorbent composed of silicate-titanate nanotubes embedded in hydrogel chitosan beads. *Environ. Technol.*
- Rahim, A.R.A., Mohsin, H.M., Thanabalan, M., Rabat, N.E., Saman, N., Mat, H., Johari, K., 2020. Effective carbonaceous desiccated coconut waste adsorbent for application of heavy metal uptakes by adsorption: equilibrium, kinetic and thermodynamics analysis. *Biomass Bioenergy* 142, 105805.
- Rajeswari, A., Amalraj, A., Pius, A., 2016. Adsorption studies for the removal of nitrate using chitosan/PEG and chitosan/PVA polymer composites. *J. Water Process Eng.* 9, 123–134.
- Rinaudo, M., 2006. Chitin and chitosan: properties and applications. *Prog. Polym. Sci.* 31, 603–632.
- Rios, C.A., Williams, C.D., Roberts, C.L., 2008. Removal of heavy metals from acid mine drainage (AMD) using coal fly ash, natural clinker and synthetic zeolites. *J. Hazard. Mater.* 156, 23–35.
- Robertson, F.N., 1989. Arsenic in ground-water under oxidizing conditions, south-west United States. *Environ. Geochem. Health* 11, 171–185.
- Romero-Perdomo, F., Beltrán, I., Mendoza-Labrador, J., Estrada-Bonilla, G., Bonilla, R., 2021. Phosphorus nutrition and growth of cotton plants inoculated with growth-promoting bacteria under low phosphate availability. *Front. Sustain. Food Syst.* 4.
- Russo, T., Fucile, P., Giacometti, R., Sannino, F., 2021. Sustainable removal of contaminants by biopolymers: a novel approach for wastewater treatment. *Curr. State Future Perspect. Process.* 9, 719.
- Sabourian, V., Ebrahimi, A., Naseri, F., Irani, M., Rahimi, A., 2016. Fabrication of chitosan/silica nanofibrous adsorbent functionalized with amine groups for the removal of Ni (II), Cu (II) and Pb (II) from aqueous solutions: batch and column studies. *RSC Adv.* 6, 40354–40365.
- Sahebjamee, N., Soltanieh, M., Mousavi, S.M., Heydarinasab, A., 2019. Removal of Cu<sup>2+</sup>, Cd<sup>2+</sup> and Ni<sup>2+</sup> ions from aqueous solution using a novel chitosan/polyvinyl alcohol adsorptive membrane. *Carbohydr. Polym.* 210, 264–273.
- Saheed, I.O., Da, O.W., Suah, F.B.M., 2020. Chitosan modifications for adsorption of pollutants – a review. *J. Hazard. Mater.* 124889.
- Saleem, A., Wang, J., Sun, T., Sharaf, F., Haris, M., Lei, S., 2020. Enhanced and selective adsorption of Copper ions from acidic conditions by diethylenetriaminepentaacetic acid-chitosan sewage sludge composite. *J. Environ. Chem. Eng.* 8, 104430.
- Saleh, H.N., Panahande, M., Yousefi, M., Asghari, F.B., Conti, G. O., Talaee, E., Mohammadi, A.A., 2019. Carcinogenic and non-carcinogenic risk assessment of heavy metals in groundwater wells in Neyshabur Plain, Iran. *Biol. Trace Elem. Res.* 190, 251–261.
- Sallam, S., El-Subrouti, G., Eltaweil, A., 2018. Facile synthesis of Ag–γ-Fe<sub>2</sub>O<sub>3</sub> superior nanocomposite for catalytic reduction of nitroaromatic compounds and catalytic degradation of methyl orange. *Catal. Lett.* 148, 3701–3714.
- Salman Tabrizi, N., Yavari, M., 2020. Fixed bed study of nitrate removal from water by protonated cross-linked chitosan supported by biomass-derived carbon particles. *J. Environ. Sci. Health Part A* 55, 777–787.
- Sandeep, A., Sangameswar, K., Mukesh, G., Chandrakant, R., Avinash, D., 2013. A brief overview on chitosan applications. *Indo Am. J. Pharm. Res.* 3, 1564–4574.
- Sani, H.A., Ahmad, M.B., Hussein, M.Z., Ibrahim, N.A., Musa, A., Saleh, T.A., 2017. Nanocomposite of ZnO with montmorillonite for removal of lead and copper ions from aqueous solutions. *Process Saf. Environ. Prot.* 109, 97–105.
- Shahnaz, T., Sharma, V., Subbiah, S., Narayanasamy, S., 2020. Multivariate optimisation of Cr (VI), Co (III) and Cu (II) adsorption onto nanobentonite incorporated nanocellulose/chitosan aerogel using response surface methodology. *J. Water Process Eng.* 36, 101283.
- Shaji, E., Santosh, M., Sarath, K., Prakash, P., Deepchand, V., Divya, B., 2020. Arsenic contamination of groundwater: a global synopsis with focus on the Indian Peninsula. *Geosci. Front.*
- Shan, H., Peng, S., Zhao, C., Zhan, H., Zeng, C., 2020. Highly efficient removal of As (III) from aqueous solutions using goethite/graphene oxide/chitosan nanocomposite. *Int. J. Biol. Macromol.* 164, 13–26.
- Shankar, P., Gomathi, T., Vijayalakshmi, K., Sudha, P., 2014. Comparative studies on the removal of heavy metals ions onto cross linked chitosan-g-acrylonitrile copolymer. *Int. J. Biol. Macromol.* 67, 180–188.
- Shao, Z., Lu, J., Ding, J., Fan, F., Sun, X., Li, P., Fang, Y., Hu, Q., 2021. Novel green chitosan-pectin gel beads for the removal of Cu (II), Cd (II), Hg (II) and Pb (II) from aqueous solution. *Int. J. Biol. Macromol.* 176, 217–225.
- Shariatinia, Z., Bagherpour, A., 2018. Synthesis of zeolite NaY and its nanocomposites with chitosan as adsorbents for lead (II) removal from aqueous solution. *Powder Technol.* 338, 744–763.
- Shebl, A., Omer, A., Tamer, T., 2018. Adsorption of cationic dye using novel O-amine functionalized chitosan Schiff base derivatives: isotherm and kinetic studies. *Desalin. Water Treat.* 130, 132–141.
- Shen, C., Chen, H., Wu, S., Wen, Y., Li, L., Jiang, Z., Li, M., Liu, W., 2013. Highly efficient detoxification of Cr (VI) by chitosan–Fe (III) complex: process and mechanism studies. *J. Hazard. Mater.* 244, 689–697.
- Sherlala, A., Raman, A., Bello, M.M., Buthiyappan, A., 2019. Adsorption of arsenic using chitosan magnetic graphene oxide nanocomposite. *J. Environ. Manage.* 246, 547–556.
- Silva, B., Martins, M., Rosca, M., Rocha, V., Lago, A., Neves, I.C., Tavares, T., 2020. Waste-based biosorbents as cost-effective alternatives to commercial adsorbents for the retention of fluoxetine from water. *Sep. Purif. Technol.* 235, 116139.
- Singha, A., Guleria, A., 2014. Use of low cost cellulosic biopolymer based adsorbent for the removal of toxic metal ions from the aqueous solution. *Sep. Sci. Technol.* 49, 2557–2567.
- Smedley, P.L., Kinniburgh, D.G., 2002. A review of the source, behaviour and distribution of arsenic in natural waters. *Appl. Geochem.* 17, 517–568.
- Sodhi, K.K., Kumar, M., Agrawal, P.K., Singh, D.K., 2019. Perspectives on arsenic toxicity, carcinogenicity and its systemic remediation strategies. *Environ. Technol. Innovat.* 16, 100462.

- Solano, R.A., De León, L.D., De Ávila, G., Herrera, A.P., 2021. Polycyclic aromatic hydrocarbons (PAHs) adsorption from aqueous solution using chitosan beads modified with thiourea, TiO<sub>2</sub> and Fe<sub>3</sub>O<sub>4</sub> nanoparticles. *Environ. Technol. Innovation* 21, 101378.
- Sowmya, A., Meenakshi, S., 2013. An efficient and regenerable quaternary amine modified chitosan beads for the removal of nitrate and phosphate anions. *J. Environ. Chem. Eng.* 1, 906–915.
- Sun, X., Yang, L., Xing, H., Zhao, J., Li, X., Huang, Y., Liu, H., 2013. Synthesis of polyethylenimine-functionalized poly (glycidyl methacrylate) magnetic microspheres and their excellent Cr (VI) ion removal properties. *Chem. Eng. J.* 234, 338–345.
- Surgutskaya, N.S., Di Martino, A., Zednik, J., Ozaltin, K., Lovecká, L., Bergerová, E.D., Kimmer, D., Svoboda, J., Sedlarik, V., 2020. Efficient Cu<sup>2+</sup>, Pb<sup>2+</sup> and Ni<sup>2+</sup> ion removal from wastewater using electrospun DTPA-modified chitosan/polyethylene oxide nanofibers. *Sep. Purif. Technol.* 247, 116914.
- Tamer, T., Abou-Taleb, W., Roston, G., Mohyeldin, M., Omer, A., Khalifa, R., Hafez, A., 2018. Formation of zinc oxide nanoparticles using alginate as a template for purification of wastewater. *Environ. Nanotechnol. Monit. Manage.* 10, 112–121.
- Tamer, T.M., Omer, A.M., Hassan, M.A., Hassan, M.E., Sabet, M. M., Eldin, M.M., 2015. Development of thermo-sensitive poly N-isopropyl acrylamide grafted chitosan derivatives. *J. Appl. Pharmac. Sci.* 5, 1–6.
- Tamer, T.M., Omer, A.M., Hassan, M.A., Hassan, M.E., Sabet, M. M., Eldin, M., 2015. Development of thermo-sensitive poly N-isopropyl acrylamide grafted chitosan derivatives. *J. Appl. Pharm. Sci.* 5, 1–6.
- Tan, Y., Wang, K., Yan, Q., Zhang, S., Li, J., Ji, Y., 2019. Synthesis of amino-functionalized waste wood flour adsorbent for high-capacity Pb (II) adsorption. *ACS Omega* 4, 10475–10484.
- Tanhaei, B., Ayati, A., Bamoharram, F.F., Sillanpää, M., 2017. Magnetic EDTA functionalized Preyssler cross linked chitosan nanocomposite for adsorptive removal of Pb (II) ions. *Clean–Soil Air Water* 45, 1700328.
- Tanhaei, B., Ayati, A., Iakovleva, E., Sillanpää, M., 2020. Efficient carbon interlayered magnetic chitosan adsorbent for anionic dye removal: synthesis, characterization and adsorption study. *Int. J. Biol. Macromol.* 164, 3621–3631.
- Upadhyay, U., Sreedhar, I., Singh, S.A., Patel, C.M., Anitha, K., 2020. Recent advances in heavy metal removal by chitosan based adsorbents. *Carbohydr. Polym.* 117000.
- Upadhyay, U., Sreedhar, I., Singh, S.A., Patel, C.M., Anitha, K., 2021. Recent advances in heavy metal removal by chitosan based adsorbents. *Carbohydr. Polym.* 251, 117000.
- Vakili, M., Deng, S., Cagnetta, G., Wang, W., Meng, P., Liu, D., Yu, G., 2019. Regeneration of chitosan-based adsorbents used in heavy metal adsorption: a review. *Sep. Purif. Technol.* 224, 373–387.
- Vickers, N.J., 2017. Animal communication: when i'm calling you, will you answer too? *Curr. Biol.* 27, R713–R715.
- Vieira, R.M., Vilela, P.B., Becegato, V.A., Paulino, A.T., 2018. Chitosan-based hydrogel and chitosan/acid-activated montmorillonite composite hydrogel for the adsorption and removal of Pb<sup>2+</sup> and Ni<sup>2+</sup> ions accommodated in aqueous solutions. *J. Environ. Chem. Eng.* 6, 2713–2723.
- Vilela, P.B., Dalalibera, A., Duminelli, E.C., Becegato, V.A., Paulino, A.T., 2019. Adsorption and removal of chromium (VI) contained in aqueous solutions using a chitosan-based hydrogel. *Environ. Sci. Pollut. Res.* 26, 28481–28489.
- Vilela, P.B., Matias, C.A., Dalalibera, A., Becegato, V.A., Paulino, A.T., 2019. Polyacrylic acid-based and chitosan-based hydrogels for adsorption of cadmium: equilibrium isotherm, kinetic and thermodynamic studies. *J. Environ. Chem. Eng.* 7, 103327.
- Wan, Z., Li, M., Zhang, Q., Fan, Z., Verpoort, F., 2018. Concurrent reduction-adsorption of chromium using m-phenylenediamine-modified magnetic chitosan: kinetics, isotherm, and mechanism. *Environ. Sci. Pollut. Res.* 25, 17830–17841.
- Wang, B., Bai, Z., Jiang, H., Prinsen, P., Luque, R., Zhao, S., Xuan, J., 2019. Selective heavy metal removal and water purification by microfluidically-generated chitosan microspheres: characteristics, modeling and application. *J. Hazard. Mater.* 364, 192–205.
- Wang, Y., Feng, Y., Zhang, X.-F., Zhang, X., Jiang, J., Yao, J., 2018. Alginate-based attapulgite foams as efficient and recyclable adsorbents for the removal of heavy metals. *J. Colloid Interface Sci.* 514, 190–198.
- Wang, L.-L., Ling, C., Li, B.-S., Zhang, D.-S., Li, C., Zhang, X.-P., Shi, Z.-F., 2020. Highly efficient removal of Cu (ii) by novel dendritic polyamine–pyridine-grafted chitosan beads from complicated salty and acidic wastewaters. *RSC Adv.* 10, 19943–19951.
- Wang, X., Zheng, Y., Wang, A., 2009. Fast removal of copper ions from aqueous solution by chitosan-g-poly (acrylic acid)/attapulgite composites. *J. Hazard. Mater.* 168, 970–977.
- Wang, X., Liu, X., Xiao, C., Zhao, H., Zhang, M., Zheng, N., Kong, W., Zhang, L., Yuan, H., Zhang, L., 2020. Triethylenetetramine-modified hollow Fe3O4/SiO2/chitosan magnetic nanocomposites for removal of Cr (VI) ions with high adsorption capacity and rapid rate. *Microporous Mesoporous Mater.* 297, 110041.
- Wang, S., Lu, Y., Ouyang, X.-K., Liang, X.X., Yu, D., Yang, L.-Y., Huang, F., 2019. Fabrication of chitosan-based MCS/ZnO@Alg gel microspheres for efficient adsorption of As (V). *Int. J. Biol. Macromol.* 139, 886–895.
- Wang, Y., Shi, L., Gao, L., Wei, Q., Cui, L., Hu, L., Yan, L., Du, B., 2015. The removal of lead ions from aqueous solution by using magnetic hydroxypropyl chitosan/oxidized multiwalled carbon nanotubes composites. *J. Colloid Interface Sci.* 451, 7–14.
- Wang, Y., Wang, Y., Wang, F., Chi, H., Zhao, G., Zhang, Y., Li, T., Wei, Q., 2022. Electrochemical aptasensor based on gold modified thiol graphene as sensing platform and gold-palladium modified zirconium metal-organic frameworks nanzyme as signal enhancer for ultrasensitive detection of mercury ions. *J. Colloid Interface Sci.* 606, 510–517.
- Wang, J., Wei, J., 2021. Facile synthesis of Zr (IV)-crosslinked carboxymethyl cellulose/carboxymethyl chitosan hydrogel using PEG as pore-forming agent for enhanced phosphate removal. *Int. J. Biol. Macromol.* 176, 558–566.
- Wang, J., Xu, W., Chen, L., Huang, X., Liu, J., 2014. Preparation and evaluation of magnetic nanoparticles impregnated chitosan beads for arsenic removal from water. *Chem. Eng. J.* 251, 25–34.
- Wang, Y., Zhou, R., Wang, C., Zhou, G., Hua, C., Cao, Y., Song, Z., 2020. Novel environmental-friendly nano-composite magnetic attapulgite functionalized by chitosan and EDTA for cadmium (II) removal. *J. Alloys Compd.* 817, 153286.
- Wang, Y., Zhao, G., Zhang, G., Zhang, Y., Wang, H., Cao, W., Li, T., Wei, Q., 2020. An electrochemical aptasensor based on gold-modified MoS<sub>2</sub>/rGO nanocomposite and gold-palladium-modified Fe-MOFs for sensitive detection of lead ions. *Sens. Actuators, B* 319, 128313.
- Wang, J., Zhuang, S., 2017. Removal of various pollutants from water and wastewater by modified chitosan adsorbents. *Crit. Rev. Env. Sci. Technol.* 47, 2331–2386.
- Wei, Y., Huang, W., Zhou, Y., Zhang, S., Hua, D., Zhu, X., 2013. Modification of chitosan with carboxyl-functionalized ionic liquid for anion adsorption. *Int. J. Biol. Macromol.* 62, 365–369.
- Wei, J., Tu, C., Yuan, G., Bi, D., Xiao, L., Theng, B.K., Wang, H., Ok, Y.S., 2019. Carbon-coated montmorillonite nanocomposite for the removal of chromium (VI) from aqueous solutions. *J. Hazard. Mater.* 368, 541–549.
- Wu, F.-C., Tseng, R.-L., Juang, R.-S., 2010. A review and experimental verification of using chitosan and its derivatives as adsorbents for selected heavy metals. *J. Environ. Manage.* 91, 798–806.
- Xu, X., Cheng, Y., Wu, X., Fan, P., Song, R., 2020. La (III)-bentonite/chitosan composite: a new type adsorbent for rapid removal of phosphate from water bodies. *Appl. Clay Sci.* 190, 105547.

- Xu, X., Ouyang, X.-K., Yang, L.-Y., 2021. Adsorption of Pb (II) from aqueous solutions using crosslinked carboxylated chitosan/carboxylated nanocellulose hydrogel beads. *J. Mol. Liq.* 322, 114523.
- Xu, Z., Wang, K., Liu, Q., Guo, F., Xiong, Z., Li, Y., Wang, Q., 2018. A bifunctional adsorbent of silica gel-immobilized Schiff base derivative for simultaneous and selective adsorption of Cu (II) and SO<sub>4</sub><sup>2-</sup>. *Sep. Purif. Technol.* 191, 61–74.
- Yan, X.-P., Kerrich, R., Hendry, M.J., 2000. Distribution of arsenic (III), arsenic (V) and total inorganic arsenic in porewaters from a thick till and clay-rich aquitard sequence, Saskatchewan, Canada. *Geochim. Cosmochim. Acta* 64, 2637–2648.
- Yang, D., Li, L., Chen, B., Shi, S., Nie, J., Ma, G., 2019. Functionalized chitosan electrospun nanofiber membranes for heavy-metal removal. *Polymer* 163, 74–85.
- Yang, S.-C., Liao, Y., Karthikeyan, K., Pan, X., 2021. Mesoporous cellulose-chitosan composite hydrogel fabricated via the co-dissolution-regeneration process as biosorbent of heavy metals. *Environ. Pollut.* 286, 117324.
- Yi, R., Cai, W., Dang, C., Han, B., Liu, L., Fan, J., 2020. Mild hydrothermal preparation of millimeter-sized carbon beads from chitosan with significantly improved adsorption stability for Cr. VI. *Chem. Eng. Res. Des.* 156, 43–53.
- Yuvaraja, G., Chen, D.-Y., Pathak, J.L., Long, J., Subbaiah, M.V., Wen, J.-C., Pan, C.-L., 2020. Preparation of novel aminated chitosan schiff's base derivative for the removal of methyl orange dye from aqueous environment and its biological applications. *Int. J. Biol. Macromol.* 146, 1100–1110.
- Zambrano-Monserrate, M.A., Ruano, M.A., Sanchez-Alcalde, L., 2020. Indirect effects of COVID-19 on the environment. *Sci. Total Environ.* 728, 138813.
- Zargar, V., Asghari, M., Dashti, A., 2015. A review on chitin and chitosan polymers: structure, chemistry, solubility, derivatives, and applications. *ChemBioEng Rev.* 2, 204–226.
- Zhang, H., Omer, A., Hu, Z., Yang, L.-Y., Ji, C., Ouyang, X.-K., 2019. Fabrication of magnetic bentonite/carboxymethyl chitosan/sodium alginate hydrogel beads for Cu (II) adsorption. *Int. J. Biol. Macromol.* 135, 490–500.
- Zhang, X., Shi, X., Ma, L., Pang, X., Li, L., 2019. Preparation of Chitosan stacking membranes for adsorption of copper ions. *Polymers* 11, 1463.
- Zhang, L., Zeng, Y., Cheng, Z., 2016. Removal of heavy metal ions using chitosan and modified chitosan: a review. *J. Mol. Liq.* 214, 175–191.
- Zhang, Y., Zhu, C., Liu, F., Yuan, Y., Wu, H., Li, A., 2019. Effects of ionic strength on removal of toxic pollutants from aqueous media with multifarious adsorbents: a review. *Sci. Total Environ.* 646, 265–279.
- Zhao, Y., Guo, L., Shen, W., An, Q., Xiao, Z., Wang, H., Cai, W., Zhai, S., Li, Z., 2020. Function integrated chitosan-based beads with throughout sorption sites and inherent diffusion network for efficient phosphate removal. *Carbohydr. Polym.* 230, 115639.
- Zhao, B., Jiang, H., Lin, Z., Xu, S., Xie, J., Zhang, A., 2019. Preparation of acrylamide/acrylic acid cellulose hydrogels for the adsorption of heavy metal ions. *Carbohydr. Polym.* 224, 115022.
- Zhao, J., Zou, Z., Ren, R., Sui, X., Mao, Z., Xu, H., Zhong, Y., Zhang, L., Wang, B., 2018. Chitosan adsorbent reinforced with citric acid modified  $\beta$ -cyclodextrin for highly efficient removal of dyes from reactive dyeing effluents. *Eur. Polym. J.* 108, 212–218.
- Zhu, C., Liu, F., Zhang, Y., Wei, M., Zhang, X., Ling, C., Li, A., 2016. Nitrogen-doped chitosan-Fe (III) composite as a dual-functional material for synergistically enhanced co-removal of Cu (II) and Cr (VI) based on adsorption and redox. *Chem. Eng. J.* 306, 579–587.
- Zou, Z., Gu, Y., Yang, W., Liu, M., Han, J., Zhao, S., 2021. A modified coagulation-ultrafiltration process for silver nanoparticles removal and membrane fouling mitigation: the role of laminarin. *Int. J. Biol. Macromol.* 172, 241–249.